THERMO-HYDRODYNAMICS OF PULSATING LAMINAR FLOW IN A MICROTUBE: A NUMERICAL STUDY

A THESIS SUBMITTED IN PARTIAL FULFILLMENT OF THE REQIUREMENTS
FOR THE DEGREE OF

Master of Technology

in

Mechanical Engineering

By

PARTHASARATHI MISHRA

ROLL NO - 212ME3313

DEPARTMENT OF MECHANICAL ENGINEERING
NATIONAL INSTITUTE OF TECHNOLOGY ROURKELA
ROURKELA-769008

JUNE-2014

THERMO-HYDRODYNAMICS OF PULSATING LAMINAR FLOW IN A MICROTUBE: A NUMERICAL STUDY

A THESIS SUBMITTED IN PARTIAL FULFILLMENT OF THE REQIUREMENTS
FOR THE DEGREE OF

Master of Technology

in

Mechanical Engineering

By

PARTHASARATHI MISHRA
212ME3313

Under the guidance of

Dr. MANOJ KUMAR MOHARANA

DEPARTMENT OF MECHANICAL ENGINEERING
NATIONAL INSTITUTE OF TECHNOLOGY ROURKELA
ROURKELA-769008

JUNE-2014

NATIONAL INSTITUTE OF TECHNOLOGY ROURKELA

CERTIFICATE

This is to certify that the thesis entitled, "**THERMO-HYDRODYNAMICS OF PULSATING LAMINAR FLOW IN A MICROTUBE: A NUMERICAL STUDY"** submitted by **Mr. Parthasarathi Mishra** in partial fulfillment of the requirements for the award of Master of Technology Degree in **Mechanical Engineering** with specialization in **Thermal Engineering** at the National Institute of Technology, Rourkela (Deemed University) is an authentic work carried out by him under my supervision and guidance.

To the best of my knowledge, the matter embodied in the thesis has not been submitted to any other University/ Institute for the award of any degree or diploma.

Dr. Manoj Kumar Moharana
Assistant Professor
Department of Mechanical Engineering
National Institute of Technology Rourkela
Rourkela– 769008

Date

SELF DECLARATION

I, Mr Parthasarathi Mishra, Roll No. 212ME3313, student of M. Tech (2012-14), Thermal Engineering at Department of Mechanical Engineering, National Institute of Technology Rourkela do hereby declare that I have not adopted any kind of unfair means and carried out the research work reported in this thesis work ethically to the best of my knowledge. If adoption of any kind of unfair means is found in this thesis work at a later stage, then appropriate action can be taken against me including withdrawal of this thesis work.

Parthasarathi Mishra

NIT Rourkela
02 June 2014

Parthasarathi Mishra

ACKNOWLEDGEMENT

I express my heartfelt sense of gratitude and indebtedness to my project guide Dr. Manoj Kumar Moharana (Assistant Professor, Department of Mechanical engineering) for his valuable and inspiring guidance towards the progress of my project topic "Thermo-hydrodynamics of pulsating laminar flow in a microtube: A numerical study".

I am also very much thankful to all my batch mates who equally share the credit in completion of project work.

I finally expressed my sincere gratitude to all those who have directly or indirectly helped me in completing this project report.

Date

Place

Parthasarathi Mishra

ABSTRACT

A two dimensional numerical analysis is carried out to understand the thermo-hydrodynamics of single phase pulsating laminar flow in a microtube with constant flux boundary condition imposed on its outer surface while the cross-sectional solid faces exposed to the surrounding are insulated. The inlet velocity to the tube is the combination of a fixed component of velocity and fluctuating component of velocity which varies sinusoidally with time, thus causing pulsatile velocity at the inlet. The working fluid is water and enters the tube at 300K. Simulations have been carried out at a range of pulsating frequency between 2-10 Hz and amplitude ratio (A) equals to 0.2. To study the effect of axial wall conduction microtube, wall to fluid conductivity ratio is taken in a very wide range (k_{sf} = 0.344 – 715) at a flow Reynolds number of 100. Effect of pulsation frequency on heat transfer is found to be very small. Heat transfer is found to be increasing at lower thermal conductive microtube wall material (or k_{sf}) while it is decreasing at higher k_{sf} compared to steady flow in microtube. Existing studies do indicate that pulsation (i) increases heat transfer (ii) decreases heat transfer, or (iii) no effect. The researchers actually failed to observe the present overall trend as none of the existing studies considered a widely varying thermal conductive wall material. Again, for a particular pulsating frequency (Wo), with very low k_{sf} leads to lower the overall Nusselt number while the time averaged relative Nusselt number remains almost constant through the entire length of microtube and it is less than the corresponding steady state Nusselt number. Higher k_{sf} with a particular frequency again lowers overall Nusselt number slightly due to severe back conduction. From this, it is confirmed that for a particular pulsating frequency, there exist an optimum value of k_{sf} which maximizes the overall Nusselt number while all other parameters like flow Reynolds number, microtube thickness to inner radius ratio (δ_{sf}) remaining the same.

KEYWORDS: Microtube, Axial Wall Conduction, Pulsatile Flow, Pulsating Frequency, Relative Nusselt number, Conductivity Ratio.

Contents

List of Figures

List of Tables

Nomenclature

A	Amplitude of pulsation
C_p	Specific heat at constant pressure, J/kg-k
D	Diameter of the tube (inner), m
f	Frequency of pulsation, Hz
h(z,t)	Instantaneous local heat transfer coefficient, W/m^2-k
k_f	Thermal conductivity of working fluid, W/m-k
k_s	Thermal conductivity of tube wall, W/m-k
k_{sf}	Ratio of k_s and k_f
L	Length of the tube, m
L_c	Characteristic length (L_c = D), m
M	Axial conduction number
Nu	Overall Nusselt number
Nu(t)	Space average instantaneous Nusselt number
Nu(z)	Time average local Nusselt number
Nu(z,t)	Instantaneous local Nusselt number
P	Gauge pressure, N/m^2
Pe	Peclet number
Po	Poiseuille number
Pr	Prandtl number ($\mu c_p/k_f$)
Q	Total heat applied at the outer surface of the tube, W
$\overline{q}$	Heat flux experienced at the solid-fluid interface, W/m^2
$\overline{q}_o$	Heat flux applied at the outer surface of the tube, W/m^2
q_z	Local heat flux experienced along the axial direction of the tube, W/m^2
r	Radial coordinate
Re	Reynold's number ($\rho UD/\mu$)
St	Strouhal number
T	Temperature, K
t	Time, s
U	Average velocity at the tube inlet, m/s
Wo	Womersley number ($L_c(\omega/\nu)^{0.5}$)
z	Axial coordinate

Greek Symbol

δ_f	Inner radius of the tube, m
δ_s	Thickness of the tube wall, m
δ_{sf}	Ratio of δ_s and δ_f
ϕ	Non dimensional heat flux
Φ	Rayleigh dissipation function
μ	Dynamic viscosity, kg/m-s
ν	Kinematic viscosity, m^2/s
θ	Time period, s
ρ	Density, kg/m^3
ω	Angular frequency, rad/s
Θ	Non dimensional temperature
∇	Differential operator

Subscript

atm	Atmospheric
av	Average
c	Central
f	Fluid
f_i	Fluid inlet
f_o	Fluid outlet
in	Inlet
out	Outlet
q	Constant heat flux boundary condition
r	Relative
s	Steady state
t	Transient/unsteady state
w	Tube wall
*	Non dimensional quantity

Chapter-1

Introduction

Recent development of electronic devices with higher processor speed needs high heat removal rate. Again as per conventional theory, heat transfer is directly proportional to the surface area and the temperature difference. While temperature difference is restricted by the application, so the surface area per unit volume is the only parameter which controls the heat transfer rate. As microtubes/microchannels having higher surface area per unit volume as compared to conventional channels is frequently used. With the development of micromachining/micromanufacturing, their applications in the field of fluid flow and heat transfer are increasing day by day. Some typical applications of micromachining in the field of fluid flow and heat transfer can be found in Khandekar and Moharana [1]. Microchannels of different sizes and shapes as per requirement can be manufactured very easily. Therefore microchannels/microtubes are gaining importance in most of the engineering applications. The relative thickness of the tube wall of a microtube compared to its inner radius leads to multi-dimensional conjugate heat transfer, depending on several other factors, i.e. thermo-physical properties of the tube wall and fluid involved, and flow conditions. Different type of flow occurs in engineering applications apart from unidirectional flow. In most of the applications flow is oscillating type.

1.1 Pulsatile flow

Conventionally, uniform fluid flow system is used in many fluid flow and heat transfer systems in conventional size as well as microchannel systems. Thus, many studies do exist in literature that deals with such systems which helped to understand the thermo-hydrodynamics of single phase as well as two-phase systems. Additionally, two more types of fluid flow that find application in many engineering systems (a) oscillating flow (or oscillatory flow), and (b) pulsating flow (or pulsatile flow). When there is no net mean velocity of the fluid in any direction and it is only oscillating back and forth about a fixed point with a superimposed frequency only then the flow is called oscillating flow .Where in case of pulsating flow, an oscillating velocity is superimposed with the one directional translational velocity. Therefore

in pulsating flow time-average velocity is non-zero whereas in oscillating flow time-average velocity is zero over any particular period of cycle at any instant. This type of flow mainly characterized by two parameters namely (i) frequency of oscillation, f (or Womersley number, Wo), and (ii) amplitude of oscillation (A). Because of rapid motion, convective heat transfer may increase in such cases. The effect of pulsations on heat transfer is an interesting problem for researchers due to its wide occurrences in many real time situations at macro as well as mini/micro level.

1.2 Applications of pulsatile flow

This type of flow frequently encountered in biological systems. Circulation of blood (Cardio vascular system) and exchange of gas through the surface of lungs (respiratory system) in human body are the best application of pulsatile flow. Cardio vascular system essentially consists of four chamber muscular organ known as heart which supplies blood to different parts of the body by the help of arteries, ventricles and capillaries. Blood circulation through the heart is entirely controlled by valve mechanisms and opening and closing of valves at specific time intervals results in periodic pulsatile flow of blood.

Similarly major components of respiratory systems are the airway, the lungs, and the muscles of respiration. The major function of airway is to transport the air between the lungs and external parts of the body. The main functional units of the respiratory system are lungs whose function is to supply oxygen into the body parts by taking carbon dioxide out of the body. Diaphragm along with intercostal muscles called as muscles of respiration which is acting as a pump, pushing air into and out of the lungs while breathing. Inhalation and exhalation are the two processes of breathing i.e. breathe in and breathe out respectively by which the body get in oxygen and expels carbon dioxide. Breathing process of lungs is mainly carried out with the help of diaphragm. At the time of breathe in or inhalation, contraction of diaphragm muscles takes place in downward direction. Thus negative pressure will created for which fresh air enters into the lungs. The situation is just opposite in case of exhalation, where expansion of diaphragm muscles takes place in upward direction, which resulted in the release of air from the lungs. So due to this contraction and relaxation of diaphragm a periodic pulsatile flow of air takes place.

Apart from biological application many engineering systems also experience pulsatile flow e.g. reciprocating engines, IC engines, pulse combustor, ramjet etc. to name a few. Pulsating flow finds extensive application in many engineering devices like pulsating heat pipes used in many thermal management applications; which is partially filled with a working

fluid. Because of its small dimension, surface tension dominates and spontaneous liquid-bubble system is generated due to the action of surface tension. This system receives heat from the evaporator section, bubble expands and liquid contracts; hence a self-sustained thermal driven oscillatory motion starts and finally transfers heat to the condenser section which lead to periodic oscillatory flow.

Similarly, many devices or systems undergo severe vibration in practical engineering applications which results in oscillatory motion of working fluids inside the systems while it moves forward. In some instance, flow is not continuous rather it oscillates due to some hurdles or obstacles in the flow direction or in the constricted passages of some complex geometry configuration devices. Apart from this, fluctuations or oscillations are sometimes associated in the flow e.g. flow over tube bundles where vortex shedding from the leading tube induces fluctuations for subsequent tubes. In many cases external pulsations are superimposed on the steady flow, example is 'pulse jet cooling'. In many industrial applications flow inside the equipment is mostly either reciprocating or pulsating type, where heat transfer takes place. Cavitation in hydraulic pipe lines and pressure surges are the most popular case of such flows in practical engineering applications.

1.3 Motivation of present work

The performances of equipment are mostly affected by the pulsating flow parameters subjected to thermal engineering applications. The convection heat transfer rate is highly dependent on the flow pulsation. The effect of pulsating flow on heat transfer is an interesting as well as challenging problem for researchers considering that this type of fluid flow occurs in natural as well as and in many engineering applications ranging from conventional to mini/micro size channels. A detail literature review regarding pulsatile flow and its effect on heat transfer is presented in next chapter. Though many studies on the effect of pulsation on heat transfer do exist in literature, they provide contradictory results. Secondly, no studies do exist in open literature that deals with study of conjugate heat transfer in pulsating flow microchannel systems. Motivation for the present work starts from the review in order to fill the gap in the literature. Hence by considering such huge application of pulsatile flow in the engineering field and gap in the literature, a dedicated study must be needed to understand the thermo-hydrodynamics of pulsating flow in order to increase the efficiency and for better thermal design of such systems.

1.4 Organization of thesis

Thesis comprises of five chapters. First chapter introduces the basics and importance of study with the problem statement. Chapter 2 gives a detailed literature review of pulsatile flow in conventional as well as microchannel systems for both laminar and turbulent flows and axial wall conduction. Chapter 3 includes problem formulation, governing equations with boundary conditions, numerical techniques, grid generation, grid selection and data reduction. Chapter 4 provides results and thermo-hydrodynamic analysis of pulsatile flow in microtube. Chapter 5 concludes the work and provides future insights.

Chapter-2

Literature review

Several researchers experimentally, analytically and numerically studied thermo-hydrodynamics of single phase pulsating flow in channels or pipes ranging from conventional to mini/micro level started working as early as in early decades of last century. So the entire literature review comprises of three sub sections:

- Pulsatile flow in conventional channel.
- Microchannel concept and axial wall conduction.
- Pulsatile flow in microchannels.

2.1 Pulsatile flow in conventional channel

Study of pulsating flow system is not new. Many researchers contributed significantly towards thermo-hydrodynamics of pulsatile flow in conventional channels. In regard to hydrodynamics behavior of pulsatile flow, Richardson and Tyler [2] did experimental study of sound waves from resonators and found that the velocity distribution of the pulsating flow in tubes of different cross-sections and sizes and confirmed the annular effect, i.e. flow velocity is maximum near the wall instead of center line of the pipe which was later verified theoretically by Uchida [3]. Uchida [3] obtained the velocity profile for the pulsating flow in a tube analytically. He assumed flow is parallel to the axis of the tube and again confirmed the annular effect [2]. The phase-lag increases with frequency and reaches an asymptotic value of 90˚ at higher frequency. In further studies [4-8], various researchers have been working on hydrodynamics of pulsatile flow and confirmed the phase-lag, annular effect and periodic axial fluctuations of temperature in pulsating pipe flow.

One significant conclusion was given by Havemann and Rao [9] on the thermal behavior of pulsatile flow. According to them heat transfer changes because pulsations alters the boundary layer thickness at each and every time stage for any particular cycle which in turn changes thermal resistance. Siegel and Perlmutter [10] considered parallel plates whose walls were subjected to uniform heat flux and uniform temperature separately. Flow inside the plate

was laminar and pulsating type and analyzed effect of pulsation frequency on heat transfer. It was found that Nusselt number showed periodic axial fluctuations when isothermal boundary condition was used. Faghri et al. [11] analytically studied heat transfer in circular duct with pulsating flow. Pulsations in velocity affects temperature distribution and divides temperature field into two parts one is steady mean part and the other one is harmonic part. They reported due to the interaction between the oscillations of velocity and temperature field, a new term comes in the energy equation which enhances heat transfer.

Karamercan and Gaine [12] experimentally investigated the effect of pulsation in a double-pipe heat exchanger and considered parameters of interest as Reynolds number, displacement amplitude, and pulsation frequency. Experiment was conducted by changing the displacement amplitude by five different values where for every flow rate the frequency of flow pulsation varied up to 300 cycles/minute. They concluded that heat transfer coefficient was increasing with pulsations, leading to higher heat transfer and the maximum enhancement was reported in the transition flow regime.

Mackley et al. [13] carried out experiment in the double tube heat exchanger by inserting baffles in the heat exchanger. Lubricating at temperature of 60^{o}C was passed on the tube side of heat exchanger which was subsequently cooled whereas shell side of the heat exchanger maintained at constant temperature by providing tap water at 11^{o}C. Pulsating mechanism provided by the help of rotary motor which was driven by cam. Temperature at different locations at different time intervals in heat exchanger was recorded by thermocouples. By changing the rotary speed oscillatory parameters was changed. From the experimental observation Mackley et al. [13] concluded that Nusselt number increases with a very reasonable manner as compared to the system where pulsation in the flow and baffles are not available.

Cho and Hyun [14] numerically studied thermo-hydrodynamics of pulsating flow in a pipe. They numerically solved unsteady laminar boundary-layer equation for wide ranges of frequency and the amplitude of oscillation. From the solution it was concluded that, Nusselt number may increase/decrease, depending on pulsating frequency but deviation of Nusselt number is very less from the steady flow.

Kim et al. [15] numerically studied hydrodynamically developed, thermally developing fluid flow in a channel with isothermal wall. Simulation was performed at Re = 50, Pr = 0.7, where the pulsation amplitude (A) and nondimensional pulsation frequency (M) taken in a wide range. From the simulation it is confirmed that when M was low, no deviation found in steady and unsteady velocity profiles. But for larger value of M, the effects of pulsation

confined to a very limited area nearer to the walls. And at the same moment, for small and moderate pulsation frequency the effect of pulsation on Nusselt number noticeable but at higher frequency the effect is negligible. The effect of pulsation on Nusselt number mainly observed in the entrance region, whereas the fully developed downstream location effect is less. Also, pressure gradient increases with frequency and at very high frequencies, flow reversal takes place for some part of pulsating phase.

Guo and Sung [16] had tested different versions of Nusselt number to clarify the conflicting results and purposed an improved version of Nusselt number which was closely matches with measurement. They found that for lower range of amplitudes, heat transfer may enhanced or reduced within a certain band of operating frequency but at higher amplitudes, heat transfer was always augmented irrespective of frequency.

Moschandreou and Zamir [17] analytically studied heat transfer characteristics in a tube subjected to constant heat flux boundary condition and observed that flow pulsation enhance the heat transfer corresponding to moderate values of frequency ranging from 5-25. The augmentations were more frequently observed at higher Prandtl number. Hemida et al. [18] obtained analytical solution for fully developed laminar pulsating flow subjected to constant wall heat flux condition and reported that the analytical solution by Moschandreou and Zamir [17] is incorrect. Hemida et al. [18] observed that heat transfer decreases under pulsating flow condition. Compared to fully developed region, the effect of pulsation was mainly observed at the thermally developing region.

Apart from these numerous numerical works, Habib et al. [19] experimentally studied the heat transfer in laminar pulsating flow in a pipe subjected constant heat flux boundary condition. Experiment was performed by varying Reynolds number (780 – 1987) and frequency of pulsation (1-29.5 Hz). Increase in relative mean Nusselt number has been reported due to the flow pulsation irrespective of the parameters. Frequency of pulsation is the major parameter affecting heat transfer whereas Reynolds number has little effect relative mean Nusselt number. From the experimental observations, it has been found for the lower range of pulsating frequency (1-4 Hz) and for Reynolds number-1366 enhancement in heat transfer was 30% from steady counterpart whereas at higher range of pulsating frequency (17-25 Hz) enhancement was up to 9% under similar condition. So in that given range of pulsating frequency relative mean Nusselt number decreased with the increase in pulsation frequency or Reynolds number. But very peculiar observation was found i.e. the relative mean Nusselt number was reduced when pulsation frequencies lies outside the range

mentioned earlier. They observed up to 40% and 20% decrease in relative mean Nusselt number for the flow frequency range of 4.1-17 Hz and 25-29.5 Hz respectively.

Another experimental study on heat transfer by pulsatile flow was carried out by Zheng et al. [20]. To introduce pulsation in flow, a self-oscillator was designed. Self-oscillator was one of the important part of the experimental setup which was essentially consists of i) inlet nozzle, ii) chamber and iii) outlet nozzle. Different experimental parameters used to control the heat transfer rate were flow rate, length of oscillating chamber and length of outlet nozzle. When very strong pulsation created by the proper adjustment of self-oscillator, maximum enhancement in heat transfer was reported whereas at weak pulsation in the flow system reduced the heat transfer rate. Due to the pulsatile flow thermal boundary layer broken at each time interval which resulted in the reduction in thermal resistance and enhancement in heat transfer rate and vice versa.

Yu et al. [21] did analytical study of laminar pulsating flow in a circular tube with constant wall heat flux, and concluded time averaged Nusselt number is not affected due to flow pulsations but the temperature and Nusselt varies periodically. Chattopadhyay et al. [22] did numerical study of pulsatile flow in a circular tube with imposed constant wall temperature boundary condition. The amplitude and frequency are varied such that $A<1.0$, and f =0-20 Hz. They observed that time-averaged heat transfer is not affected due to flow pulsation, although the Nusselt number fluctuates with time in the developing region of the pipe.

Many researchers have tried to explore the effect of pulsation on heat transfer for single phase turbulent flow in a pipe. Out of them, in 2007 Elshafei et al. [23] numerically investigated pulsatile flow in turbulent air flow in a pipe which was subjected to constant heat flux boundary condition by Fluent code. Reynolds number was ranging from (10^4 to 4×10^4) while the pulsation frequency was taken at a wider range (0-70 Hz). The local time-averaged Nusselt number may increase or decrease corresponding to its steady flow values depending on either the frequency or the Reynolds number. At higher pulsating frequency, mean time-averaged Nusselt number was little affected by the variation of frequency. At very small value of pulsation frequency, the heat transfer coefficient was changed an appreciable amount by the variation of pulsating frequency. However, heat transfer rates little affected by changing pulsating frequency. For a particular range of pulsating frequency ($f \leq 39.34$ Hz and for $f \geq 42.5$ Hz) meantime averaged Nusselt number never increased and little increased at Reynolds number (Re =22.5 × 10).

Elsayed et al. [24] carried out experimental investigation on similar problem studied by Elshafei et al. [23]. Experimental procedure of laminar pulsating flow was almost similar to the one by Habib et.al. [19]. The experiments was performed by varying in the same range of Reynolds number as Elsayed et al. [23] while frequency of oscillation was kept in a range of 6.6 to 68 Hz. For introducing pulsatile flow an oscillator was installed in the tube exit. From the experimental results it has been found that heat transfer rate was mainly depends on both the variables (pulsating frequency, Reynolds number). Depending on the values of the variables, the Local Nusselt number may increase/decrease. Higher values of Nu reported near the inlet of the tube. The maximum increase in average relative enhancement ratio of local heat transfer coefficient was 9% at Re = 37,100, f = 13.3 Hz. Maximum decrease (12%) also reported at Re = 13,350, f = 42.5 Hz.

Mehta and Khandekar [25] numerically studied heat transfer characteristics of pulsating flow in a circular axisymmetric tube where both one directional flow, pulsations subjected in axial direction and in a parallel plate where one directional flow is associated with transverse pulsation. They observed effect of frequency (Womersley number, Wo), Prandtl number (Pr), Reynolds number (Re) and amplitude ratio (A) on the instantaneous and time averaged heat transfer and friction factor (Po). Effect of Wo, Re and A on time averaged Nusselt number was not appreciable while increase in Prandtl number leads to reduction in time averaged relative Nusselt number. In case of circular tube no enhancement in heat transfer was observed, while in case of parallel plates, enhancement in time average Nusselt number was found in the developing zone for smaller spacing ratio and larger frequency. Deviation of Nusselt number from the steady counterpart was very negligible in the fully developed flow regions whereas the effect is more clearly observed in the developing region for the case of both circular duct and parallel plates.

Jafari et al. [26] numerically studied the effects of flow pulsation in a corrugated channel. The simulation was carried out at Pr = 3.103 and different Re (50, 100 and 150) where the dimensionless frequency (i.e. Strouhal number, St) and oscillatory amplitude (A) were taken at a broad range ($0.05 \leq St \leq 1$, $0 \leq A \leq 0.25$). Pulsating velocity is the key parameter affecting heat transfer enhancement. It was found that for a particular Strouhal number known as extemum value of Strouhal number (which again dependent on Reynolds number), heat transfer is maximum and at higher frequency heat transfer rate decreases. Heat transfer rate was increased linearly with amplitude of oscillating velocity and more prominent at extreme value of Strouhal number. Results also indicated that the flow pulsation has better thermal performance at higher Reynolds numbers.

Afrouzi et al. [27] numerically investigated the effect of flow pulsation on the heat transfer in a single helical tube under isothermal wall boundary condition. The effect of pulsation amplitude and frequency, tube pitch and tube helix ratio on the Nusselt number was investigated. Pulsating frequency has considerable effect on heat transfer. By increasing frequency of pulsation, average Nusselt number increases whereas pitch of helix has no effect on the heat transfer characteristics. The average Nusselt number decreases by increasing of helix ratio at constant amplitude and increases by the increasing of amplitude at constant helix ratio.

Although many literatures are available in relation to pulsatile flow in conventional channels [9-27], but no significant conclusion is drawn regarding the effect of pulsation on heat transfer. A very first question comes to mind in pulsating convection heat transfer; does superimposed pulsation enhances or reduces heat transfer over the original steady state? It is very difficult to answer this question, since the existing literatures provide very diverging answers i.e. i) pulsation enhances heat transfer [9, 11-13, 20] ii) it reduces heat transfer [18] iii) it does not effect on heat transfer [10, 21, 22, 25] iv) it either increases or decreases heat transfer depending on certain parameters [14-17, 19, 23-24, 26-27].

2.2 Microchannel concept and axial wall conduction

With developments in micro-manufacturing technology, many applications of fluid flow and heat transfer in mini/microchannels has emerged. Typical applications include cooling of miniaturized devices, Bio-fluidic systems etc. to name a few. Micro heat exchangers play a vital role in the thermal management of many engineering devices. Axial wall conduction play crucial role in thermal performance of micro heat exchangers. Axial wall conduction is not a new concept and is not confined to microchannels only. Axial wall conduction also exists in conventional channels but in most cases its magnitude is negligible, due to the smaller wall thickness as compared to inner radius. Therefore, the whole attention is focused on recent studies in this field.

A detailed review on axial wall conduction in microchannels is available in [28-39]. Maranzana et al. [28] carried out both analytical and numerical investigation in order to visualize the effects of axial heat conduction phenomena in the walls of a mini/micro channel. They introduced a new non dimensional number i.e. axial conduction number (M)

$$M = \frac{q_{conductive}}{q_{convective}} = \left(\frac{k_s \frac{\delta_s w}{L}}{\rho C_p \delta_f w U_{av}} \right) \qquad (2.1)$$

They concluded that the effect of axial conduction in the walls of mini/microchannels is negligible if M<0.01 and it cannot be neglected if M>0.01.Their analysis was based on the assumption that the temperature difference between the inlet and outlet location of the solid wall in the axial direction (ΔT_w) and in the axial direction of the fluid (ΔT_f) domain was same. But in actual practice, the above assumption is wrong.

To overcome the limitations in Maranzana et al. [28], Zhang et al [29] considered temperature difference between inlet and outlet location of the solid and fluid domain. They numerically investigated effects of axial wall conduction in a thick microtube subjected to constant temperature on the outer wall. From the conjugate heat transfer study by Zhang et al. [29] it has been found that axial heat conduction depends on many parameters and geometric conditions.

Both numerical and analytical analysis was carried out by Cole and Cetin [30] in order to understand the effect of axial wall conduction in a parallel-plate microchannel subjected to uniform heat flux at the outer wall. They observed that axial wall conduction along the channel wall becomes dominating at (a) smaller length of microchannel over height ratio (b) small Peclet number (c) higher wall thickness to channel height ratio, and (d) high thermal conductive wall material in compares to thermal conductivity of the working fluid. On the mean time, the effect of the axial wall conduction in the wall was neglected for high Peclet number (e.g. Pe > 100) or lower thermal conductive wall material.

Moharana et al. [31] did a combined experimental and numerical study to explore axial wall conduction in minichannel array and observed that due to axial wall conduction in the solid substrate, the experimental setup is likely to have conjugate effects at higher value of the axial conduction number. This result in reduction in local experimental Nusselt numbers and also their axial variation is affected. They concluded that geometry and flow conditions are going to decide dominance of conjugate heat transfer effects in mini/microchannels.

Moharana et al. [32] numerically studied axial wall conduction in circular tube and square shaped microchannel on a solid substrate over a broad range of Reynolds number, conductivity ratio and thickness of wall. They observed that the conductivity ratio is one of the key factor in controlling the extent of axial conduction on the heat transport characteristics at the solid-fluid interface. For constant wall heat flux boundary condition, Moharana et al. [32] found that there exists an optimum value of solid to fluid conductivity ratio at which the average Nusselt number is highest.

Moharana and Khandekar [33] numerically studied axial wall conduction in microtube subjected to constant wall temperature boundary condition. Although the work was similar to Moharana et al. [32], but conclusion was different. They never found such an optimum solid to fluid conductivity at which heat transfer is maximum as in [32], rather reported by increasing conductivity ratio average Nusselt number decreases.

Rahimi and Mehryar [34] numerically investigated variation of local Nusselt number along the two ends of circular micro pipe subjected to constant heat flux at its wall. Simulation was carried out for different Re, Pr, and with variable geometry. It has been observed that the axial wall conduction in the pipe wall strongly influenced by the thermal conductivity of wall and wall thickness, which results in the decrease and deviation in the local Nusselt number along the entry and ending region of the micro pipe respectively.

A three dimensional rectangular microchannel with constant heat flux at the bottom wall of the substrate was considered in the numerical simulation of Moharana and Khandekar [35]. In the analysis substrate of fixed size (0.6 mm × 0.4 mm × 60 mm) was selected and channel aspect ratio was changed from 0.45 to 0.4 by independently varying width and height (w/h) of the channel. From their numerical simulation it has been found that the channel aspect ratio also plays some role in the conjugate heat transfer in microchannels.

Tiwari et al. [36] numerically studied axial wall conduction in a partially heated microtube with constant heat flux over a wide range of wall to fluid conductivity ratio, thickness ratio and Reynolds number. Also the results were compared with fully heated microtube and observed optimum conductivity ratio at which average Nusselt number is maximum similar to Moharana et al. [32]. Kumar and Moharana [37] extended the work of Tiwari et al. [36] under constant wall temperature boundary condition and found average Nusselt number is decreasing by increasing thickness ratio except at very low thermal conducive material in case of partial heated microube.

Hasan et al. [38] numerically studied axial heat conduction in a three dimensional isosceles right triangular microchannel heat exchanger. Analysis was carried out with the assumptions i.e. flow is laminar, incompressible, single-phase, and steady state. It has been shown from the result, axial heat conduction plays an important role in a parallel flow microchannel heat exchanger and was greatly affected by different parameters like i) Reynolds number (Re) ii) Ratio of thermal conductivity of wall to fluid (k_{sf}), iii) hydraulic diameter (D_h) iv) thickness of separating wall (δ_s) and v) channel volume. Axial heat conduction was increased by increasing Re, k_{sf} and δ_s while it decreased by increasing hydraulic diameter and channel volume.

Recently, Lin and Kadilikar [39] experimentally studied axial wall conduction and scale effects in different stainless microtubes of 962, 308, and 83 μm inner diameters with air as the working fluid. The experimental gas flow loop consisted of an air bottle, a regulator, and three flow meters. The temperature and pressure drop of the air was measured with a resistance temperature detector and pressure transduce. The wall temperature of the microtubes was measured by LCT and thermocouples. In small diameter tubes viscous heating effects were more pronounced and these effects enhanced by increasing Reynolds number (Re). Axial heat conduction causes an underestimation of Nusselt number and the magnitude of deviation increases with decreasing Re, increasing tube wall thickness, and increasing tube wall material thermal conductivity.

2.3 Pulsatile flow in microchannels

Many researchers [28-39] studied the effect of axial wall conduction in microchannel systems but considered steady flow of coolant. Apart from constant velocity flow, involvement of oscillating type of flow is more pronounced in most of the engineering applications as well as in mini/microchannel systems. Very few numbers of studies is available in the open literature, [40-45] which basically deals with the analysis of pulsating flow in microchannel systems.

Persoons et al. [40] experimentally investigated the effect of steady as well as pulsatile flow in microchannel heat sinks. To provide pulsatile flow pulsatile flow a pulsatile flow generator used which was adjustable with frequency and amplitude, essentially consists of i) check valves, ii) pumping chambers and iii) piezoceramic actuator disk. Experiments were carried out for different range of parameters namely steady, pulsating Reynolds number and Womersley number for single microchannel geometry. From the investigated range of parametric variations, experimental results showed the increase in overall heat transfer compared to the steady flow case. Enhancement factors $[(Nu_t-Nu_s)/Nut]$ reported as 40%. For small pulsation amplitude ($Re_p/Re<0.2$) negligible increase and sometimes decrease in Nusselt number whereas for large pulsation amplitudes ($Re_p/Re>0.2$) always enhancement in heat transfer was reported.

Analysis of blood flow in channels of dimensions of the order of tens to hundreds of microns is similar to the pulsatile flow in microchannel. Blood flow in arterioles, venules and fine capillaries in human body are the best examples of such case. Due to the development of several lab-on-chip devices in biomedical application, it is very essential to study the mechanics of blood flow through such channel.

In this regard, a significant contribution was given by Kumar and Agrawal [41]. They experimentally analyzed blood flow in a microchannel over broad range of hydraulic diameters varying from 70-1000 μm. Experimental set up essentially consists of set of microchannels, Pressure gauge and peristaltic pump which causes pulsatile variation of blood. They basically measured pressure drop, f·Re for round and trapezoidal cross section microchannel. Apart from this, variation of relative viscosity with strain rate for different cross section channels has been reported.

Tikekar et al. [42] experimentally studied pulsatile flow in microchannel of dimension (260μm×100μm×20mm) and hydraulic diameter corresponds to 144 μm. Experimental setup essentially consists of pressure gauge to measure at the input of microchannel, damper, flow splitter, and a micropump whose function is to supply of working fluid (deionized water) from the reservoir. They basically measured the pressure drop with time across the microchannel over wide range of parameters. They conducted experiments by varying flow rate, pulsation frequency, and duty cycle over a wide range.

Persoons et al. [43] carried out the same experiment as conducted by Persoons et al. [40] but at a wide range of parametric variation. Reynolds number and Womersley number were taken in the range of 100 to 650 and 6 to 17 respectively, while the ratio of pulsating to steady Reynolds number kept between 0.002-3. Analogous observation was found as reported by Persoons et al. [40]. Effect of Womersley number on heat transfer was very negligible in the given range.

Nandi and Chattopadhyay [44] extended the work of Chattopadhyay et al. [22] over microchannels and verified the pulsation effects. In the inlet of microchannel pulsatile velocity was introduced which varies sinusoidally with time and the channel wall subjected to uniform temperature. Simulation was carried out for different range of Reynolds number, dimensionless frequency and amplitude of pulsation. By comparing results with steady flow simulation it has been concluded that pulsation has appreciable effect at lower Reynolds number (nearly 20) beyond which the effect is neglected.

Again Nandi and Chattopadhyay [45] did the similar work correspond to [44] by considering a two dimensional wavy microchannel. Numerical simulation was done for Prandtl number 7 and Reynolds number ranging from 0.1- 100 similar to [44]. They studied the effect of pulsation by comparing the results with corresponding steady flow. From the results of numerical simulation, it has been found wavy channel show better thermal performance at different amplitude (0.2, 0.5, and 0.8) and frequency (1, 5, and 10).

From review of literature, it is revealed that some researchers mainly focused on hydrodynamics of pulsatile flow [2-8] and many studies on the effect of pulsation on heat transfer do exist in literature, they provide contradictory results [9-27]. All the existing and recent studies on effect of axial wall conduction in microchannel systems considered steady flow of coolant [28-39]. Secondly, no studies do exist in open literature that deals with study of conjugate heat transfer in pulsating flow microchannel systems. Few researchers have considered pulsating flow in microchannels [40-45] but they either considered only pressure drop [41-42] or neglected conjugate heat transfer [40,43-45].

In this background, a two-dimensional numerical study has been carried out in Ansys-Fluent® platform to study conjugate heat transfer in pulsating flow in a microtube subjected to constant wall heat flux. This will help in proper understanding of thermo-hydrodynamics of pulsating flow in mini/microchannels.

Chapter -3

Numerical simulation

3.1 Problem formulation

A microtube with inner radius (δ_f), tube thickness (δ_s) and length (L) has been considered as shown in Fig. 1(a). Water is used as the working fluid and enters the microtube at 300 K (Pr = 7) with a slug velocity that varying with time sinusoidally, thus causing pulsating flow in the microtube. The inlet velocity (U_{in}) thus consists of a fixed component (U_{av}) and a fluctuating component ($U_{av} \cdot A \cdot \sin(\omega t)$) which varies sinusoidally with time. Due to axisymmetry, a two-dimensional computational domain is considered as shown in Fig. 1(b). This helps in saving computational time. The thickness (δ_s), inner radius (δ_f), length (L) of the microtube are kept constant in the computational model at 0.2 mm, 0.2 mm, and 60 mm respectively. The sinusoidal curve for pulsatile flow magnitude is also shown below, where the values near different points indicated on the curve represents the phase angle in degree.

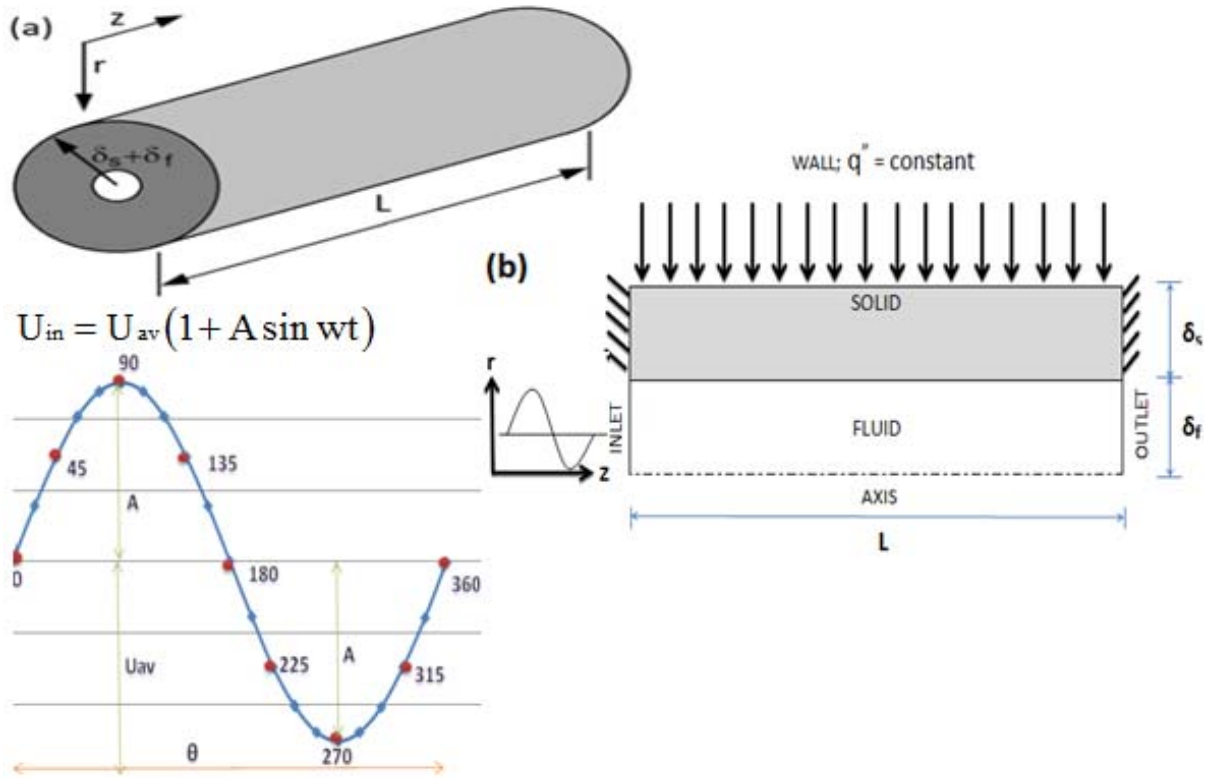

Fig. 3.1: Microtube and its computational domain with pulsating velocity at inlet.

3.1.1 Assumption

Numerical analysis has been carried out with the following prior assumptions:

- Flow is laminar, incompressible, and in single phase.
- Thermo-physical properties of the fluid are constant.
- Heat transfer through natural convention and radiation mode is negligible.

3.1.2 Governing equations

The flow and heat transfer are governed by the Navier-Stokes and energy equations. Hence time dependent, incompressible two-dimensional governing equations with constant thermo-physical properties in axisymmetric cylindrical coordinate system can be written as:

Continuity equation:

$$\frac{1}{r}\frac{\partial(rv)}{\partial r}+\frac{\partial u}{\partial z}=0 \tag{3.1}$$

Navier-Stokes equation:

$$\text{z direction}: \quad \frac{\partial u}{\partial t}+v\frac{\partial u}{\partial r}+u\frac{\partial u}{\partial z}=-\frac{1}{\rho}\frac{\partial p}{\partial z}+\nu\left(\frac{1}{r}\frac{\partial}{\partial r}\left(r\frac{\partial u}{\partial r}\right)+\frac{\partial^2 u}{\partial z^2}\right) \tag{3.2}$$

$$\text{r direction}: \quad \frac{\partial v}{\partial t}+v\frac{\partial v}{\partial r}+u\frac{\partial v}{\partial z}=-\frac{1}{\rho}\frac{\partial p}{\partial r}+\nu\left(\frac{1}{r}\frac{\partial}{\partial r}\left(r\frac{\partial v}{\partial r}\right)+\frac{\partial^2 v}{\partial z^2}-\frac{v}{r^2}\right) \tag{3.3}$$

Energy equation:

$$\rho c_p\left(\frac{\partial T}{\partial r}+v\frac{\partial T}{\partial r}+u\frac{\partial T}{\partial z}\right)=k\left(\frac{1}{r}\frac{\partial}{\partial r}\left(r\frac{\partial T}{\partial r}\right)+\frac{\partial^2 T}{\partial z^2}\right)+\mu\Phi \tag{3.4}$$

where Φ is known as Rayleigh dissipation function.

3.1.3 Boundary condition

For solid domain, $\nabla^2 T=0$ (3.5)

At $z=0$ to $z=L$ and $r=0$, $\frac{\partial U}{\partial r}=0$ (3.6)

At $z=0$ and $r=0$ to $r=\delta_f$, $U_{in}=U_{av}(1+A\sin\omega t)$; $T_{in}=T_{atm}$ (3.7)

At $z=L$ and $r=0$ to $r=\delta_f$, $P=0$ (3.8)

At $z=0$ and $r=\delta_f$ to $r=\delta_s+\delta_f$, $\frac{\partial T}{\partial z}=0$ (3.9)

At $z=L$ and $r=\delta_f$ to $r=\delta_s+\delta_f$, $\frac{\partial T}{\partial z}=0$ (3.10)

At $z=0$ to $z=L$, $r=\delta_s+\delta_f$, $q=\text{const}$ (3.11)

3.2 CFD modelling

The governing equations (i.e. continuity, Navier-Stokes and energy equations) are solved using commercially available Ansys Fluent-13.0 which is based on finite volume discretization.

3.2.1 Geometry creation

The computational domain of the microtube (L = 60 mm and R = 0.4 mm) can be taken as two dimensional rectangle (as shown in Fig. 3.1(b)) due to axi-symmetry. For the creation of above geometry in Ansys13.0 workbench on the toolbox Fluid flow (Fluent) was selected. Then analysis type is changed from 3D to 2D by selecting property at the Geometry level. In the DESIGN MODLER (DM) screen 'mm' as the unit was chosen. Then two rectangles were sketched and dimension was specified in the ZY plane. Surfaces were created from the sketching with proper naming. After generation of surfaces body type was defined i.e. inner rectangle as FLUID and the outer rectangle as SOLID. For achieving of coupled condition for conjugate heat transfer between two surfaces, one part with two surfaces was formed by selecting both surfaces and by clicking on to form NEW PART. After naming the boundaries of the computational domain as (Symmetry, Conjugate wall, Top wall, Insulated wall 1, Insulated wall 2, Inlet, and Outlet), the geometry was saved.

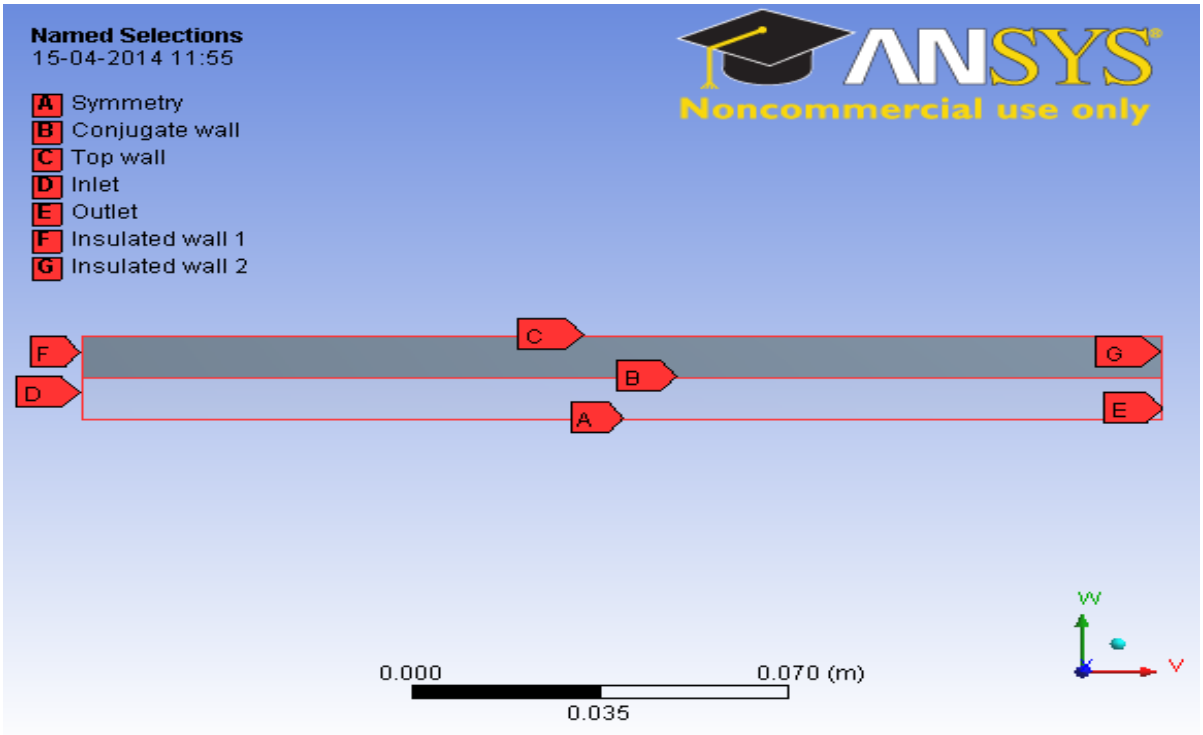

Figure 3.2: Computational domain with named boundary

3.2.2 Grid generation

Since quality, number and structure of grid are the three major parameters which will affect the accuracy label of a computational problem, grid generation presents one of the major steps in numerical solutions. After creation of geometry DESIGN MODLER screen was closed and MESH was selected on Project Schematic screen. Immediately a separate Meshing window opened and GENERATE MESH bottom was selected. By so, default meshes were created throughout the domain which further modified with the help of MESH CONTROL. EDGE SIZING was done in MESH CONTROL option by selecting QUAD as the meshing method, number of divisions on each edge and HARD as type of grid. For generating grid throughout the face of the domain, MAP facing was done by selecting MAPPED FACE bottom. Since boundaries mostly affected in computational procedure, finer and smoother meshes were generated at the boundaries of the domain for easy and smooth transmission of properties from one grid to other leading to the increase in accuracy level. Zoomed view of the grid structure shown below.

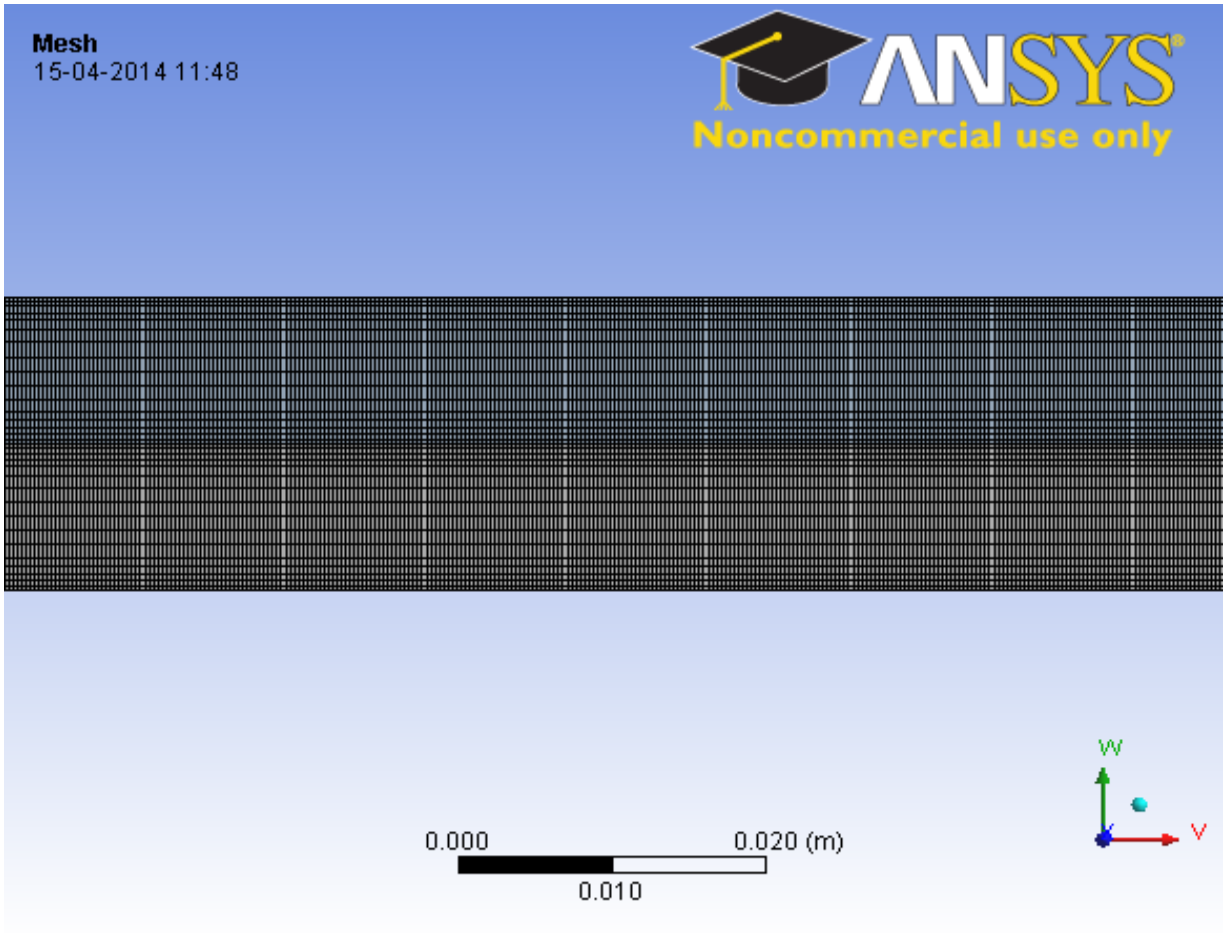

Figure 3.3: Structure of grid in computational domain

3.2.2.1 Grid independence test

Grid independence test was carried out to confirm the grid size. As an example, grid independence test of a microtube with negligible wall thickness subjected to constant wall heat flux at the wall and pulsatile velocity at the inlet was performed for both central line velocity (U_c) and instantaneous local Nusselt number [Nu(z,t)] shown in Fig. 3.4 (a) and (b) respectively by considering different number of grids described below.

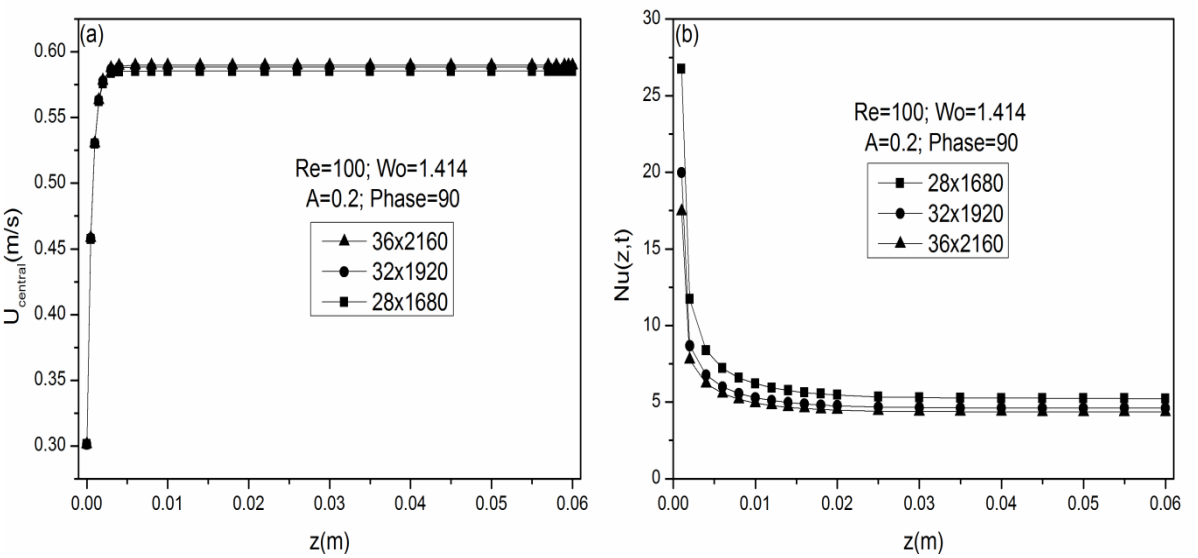

Figure 3.4: Grid independence test

In Fig. 3.4(a), center line velocity (U_c) for a particular phase angle (90) is plotted for three different mesh sizes of 28×1680, 32×1920, and 36×1080 for the given microtube. It can be shown that when grid size increases from 28×1680 to 32×1920 there is no increment in central line velocity (U_c) in the developing region where as in the fully developed region there is slight increment (0.51%) observed. By further increasing grid size from 32×1920 to 36×2160, there is very little increment (0.12%) in center line velocity in the fully developed region.

Figure 3.4(b) shows the instantaneous local Nusselt number for a particular phase angle (90) at three different mesh sizes of 28×1680, 32×1920, and 36×1080. By increasing grid size from 28×1680 to 32×1920, instantaneous local Nusselt number [Nu(z,t)] decreased by 5.38%. By further increasing grid size from 32×1920 to 36×2160, the percentage difference instantaneous local Nusselt number [Nu(z,t)] is reduced to 0.935.

Based on the results of grid independence test, for both central line velocity and instantaneous local Nusselt number, it is confirmed that '32×1920' is the proper grid size and used for the simulation.

3.2.3 Setup and flow specification

The given meshed geometry exported to the fluent setup where physical and flow properties specified. In the problem setup pressure based solver and absolute velocity formulation was maintained as the default setting. Unsteady time and axisymmetric 2D space as the solver type was set in the general menu. Energy equation was turned on, while all other models remain as it is. In the material section water was chosen as the working fluid whose thermo-physical properties mentioned below:

Table 3.1: Thermo-physical properties of water

Property	**Symbol**	**Value**	**Unit**
Specific heat at constant pressure	C_p	4182	J/kg-K
Thermal conductivity	k_f	0.6	W/m-K
Dynamic viscosity	μ	0.001003	Kg/m-s
Density	ρ	998.2	Kg/m^3

After selecting working fluid with proper thermo-physical property, different solid materials were set separately in the material section as the microtube wall material whose properties are listed in a table below:

Table 3.2: Thermo-physical properties of different microtube wall materials

Solid Name	**ρ (Kg/m^3)**	**C_p (J/kg-K)**	**k_s (W/m-K)**	**k_{sf} (k_s/k_f)**
Sulfur	2070	708	0.206	0.344
Silicon dioxide	2220	745	1.38	2.3
Bismuth	9780	122	7.86	13.1
Nicrome	8400	420	12	20
SS316	8238	468	13.4	22.33
Constantan	8920	384	23	38.34
Chromium steel	7822	444	37.7	62.84
Bronze	8780	355	54	90
Zink	7140	389	116	193.33
Aluminum	2719	871	202.4	337.33
Copper	8978	381	387.6	646
Silver	10,500	235	429	715

After the selection of the materials for both fluid and solid, cell zone condition at part 1 was changed from air to water. To provide pulsatile flow at the tube inlet user defined function (UDF) in C programming language was interpreted. Then the boundary conditions at inlet, outlet and walls were defined.

3.2.4 Solution

'Implicit integration' solution method was used for temporal discretization. 'Green-Gauss cell based' theorem was used to compute scalars at the cell centers. 'SIMPLE' algorithm was used for pressure velocity coupling, 'Second order upwind scheme' used for discretization of momentum and energy equations. Pressure interpolation was done using 'standard' scheme. Solution control parameters i.e. under relaxation factors were kept as default values listed below:

Table 3.3: Value of under relaxation factors

Pressure	Density	Body forces	Momentum	Energy
0.3	1	1	0.7	1

Absolute convergence criterion for momentum and energy was set at 10^{-5} and 10^{-9} respectively. A scaled residuals monitor for a specific case of the given problem attached below (Fig. 3.5) where the solution was converged for each time-step. '250-350' no of iterations needed for the convergence of local variables at each time step.

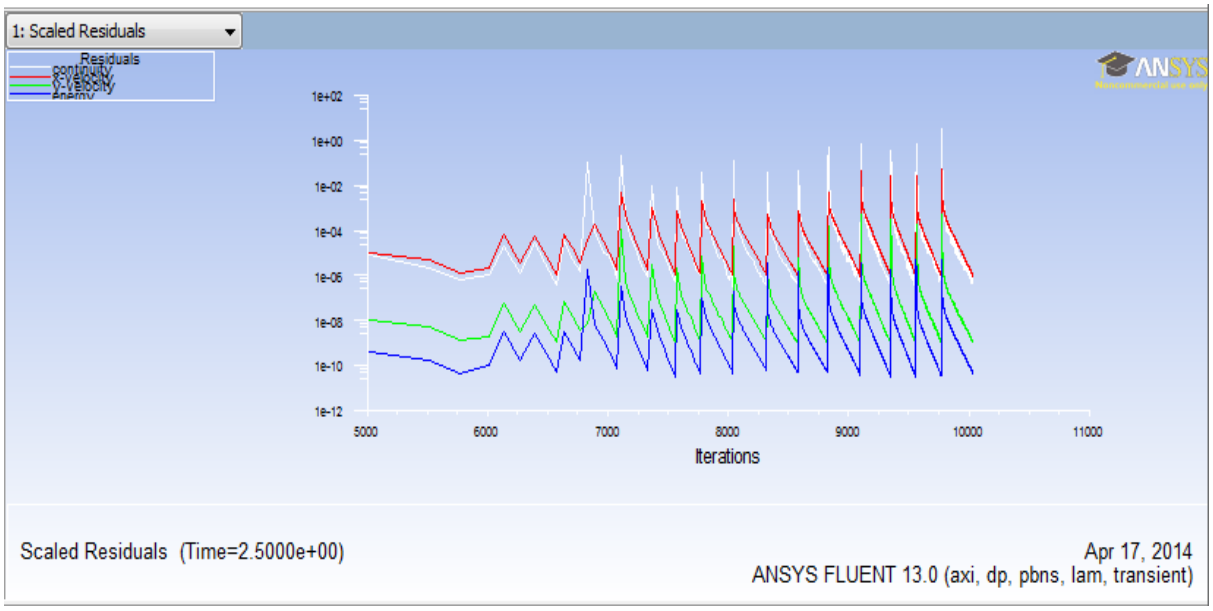

Fig. 3.5: Monitoring of scaled residuals

Standard initialization was used for solution initialization and computed from the inlet. For the extraction of data at different time step of any cycle, auto save option was set for every time step during iteration. Under run calculation, time stepping method was maintained as fixed. Maximum iteration per time step was set 1000 while local variables converged nearly '250-300' number of iterations in each time step. Reporting interval and profile update interval were kept as the default value i.e. 1. Time step size was calculated from the frequency of pulsation and number of time steps so maintained that steady periodic solution is obtained.

3.3 Data reduction

The parameters of interest are (a) local heat flux at different phase angle of pulsation for a particular cycle (b) local wall temperature at different phase angle of pulsation for a particular cycle (c) local bulk fluid temperature at different phase angle of pulsation for a particular cycle. These parameters allow us to determine extent of axial conduction over the instantaneous local Nusselt number where conductivity ratio (k_{sf}) plays a very vital role.

Axial coordinate (z) in dimensionless form is defined as

$$z^* = \frac{z}{L} \tag{3.12}$$

The heat flux applied to the outer surface of the microtube

$$\bar{q}_0 = \frac{Q}{2 \cdot \pi \cdot (\delta_s + \delta_f) \cdot L} \tag{3.13}$$

where Q is the total heat applied on the outer surface of the microtube. The ideal heat flux at solid-fluid interface is

$$\bar{q} = \bar{q}_0 \frac{\delta_s + \delta_f}{\delta_f} \tag{3.14}$$

The non-dimensional local heat flux at solid- fluid interface is

$$\phi = \frac{q_z}{\bar{q}} \tag{3.15}$$

where q_z is the actual local heat flux experienced at the solid-fluid interface along the axial direction of the microtube. The dimensionless bulk fluid and microtube wall temperature, which varies along the axial direction are given by

$$\Theta_f = \frac{T_f - T_{fi}}{T_{fo} - T_{fi}} \tag{3.16}$$

$$\Theta_w = \frac{T_w - T_{fi}}{T_{fo} - T_{fi}} \tag{3.17}$$

where, T_{fi} and T_{fo} are the average bulk fluid temperature at the inlet and outlet of the microtube respectively, T_f is the average bulk fluid temperature at any location z, and T_w is the microtube wall temperature at the same location.

The instantaneous local Nusselt number is:

$$Nu(z,t) = \frac{h(z,t) \cdot D}{k_f} \tag{3.18}$$

where h(z,t) is the instantaneous local heat transfer coefficient and is given by

$$h(z,t) = \frac{q_z}{T_w - T_f} \tag{3.19}$$

The space average instantaneous Nusselt number is given by

$$Nu(t) = \frac{1}{L}\int_0^L Nu(z,t)\,dz \tag{3.20}$$

and the time average local Nusselt number over a single cycle is given by

$$Nu(z) = \frac{1}{\theta}\int_0^\theta Nu(z,t)\,dt \tag{3.21}$$

The overall Nusselt number is given by

$$Nu = \frac{1}{\theta L}\int_0^L\int_0^\theta Nu(z,t)\,dt\,dz \tag{3.22}$$

Relative Nusselt number is given by

$$Nu_r = \frac{Nu_t}{Nu_s} \tag{3.23}$$

where Nu_t and Nu_s are the Nusselt number corresponding to transient and steady state respectively.

Chapter-4

Results and discussion

The average flow Re (based on mean velocity over a cycle) is maintained at 100. Water is used as the working fluid and enters the microtube at 300K (Pr = 7) with a slug velocity that varying with time sinusoidally. For the steady periodic solution, all analysis is done for a particular cycle (7^{th} cycle) at different phase angles ranging from 0-360.

Hydrodynamic analysis of pulsatile flow is carried out under ideal condition (zero wall thickness). Initially, verification of UDF is done with the theoretical results for different phase angles and amplitude of oscillations over a period of cycle. Verification is carried out for a particular pulsation frequency (f) is i.e. 2 Hz which corresponds to Wo = 1.414 whereas amplitude of pulsation (A) is varied from 0.2 to 0.4. From the verification, it has been found that theoretical results are in good agreement with the numerical results by UDF programming.

Radial variation of velocity for different phase angles at a particular location in the fully developed region is shown in Figs. 4.1 and 4.2 respectively. From the Fig. 4.1 and Fig. 4.2, it is confirmed that, when the phase angle is 270 the velocity is lowest and when the phase angle is 90, velocity is highest which is also theoretically correct. At the phase angle 135, velocity is higher from the velocity corresponding to phase angle 45 in the nearer to central region of the tube whereas situation is just reverse nearer to the wall i.e. velocity corresponding to phase angle 45 is more than the velocity corresponding to phase angle 135. Analogous observation is found for the phase angle 225 and 315 which is clearly shown in Fig. 4.2. Due to the effect of inertia this small deviation in velocity is reported. Again from the Fig. 4.2, it is clear that the velocity profiles overlaps for three different phase angles (0,180,360). Increase in velocity is reported for the positive half cycle with phase angles ranging from 45-135, by changing the amplitude of pulsation from 0.2 to 0.4. And at the same time decrease in velocity due to pulsation is reported for negative half cycle with phase angles ranging from 225-315 by increasing the amplitude ratio in the same range taken earlier. (See Fig. 4.1. (a)-(f)).

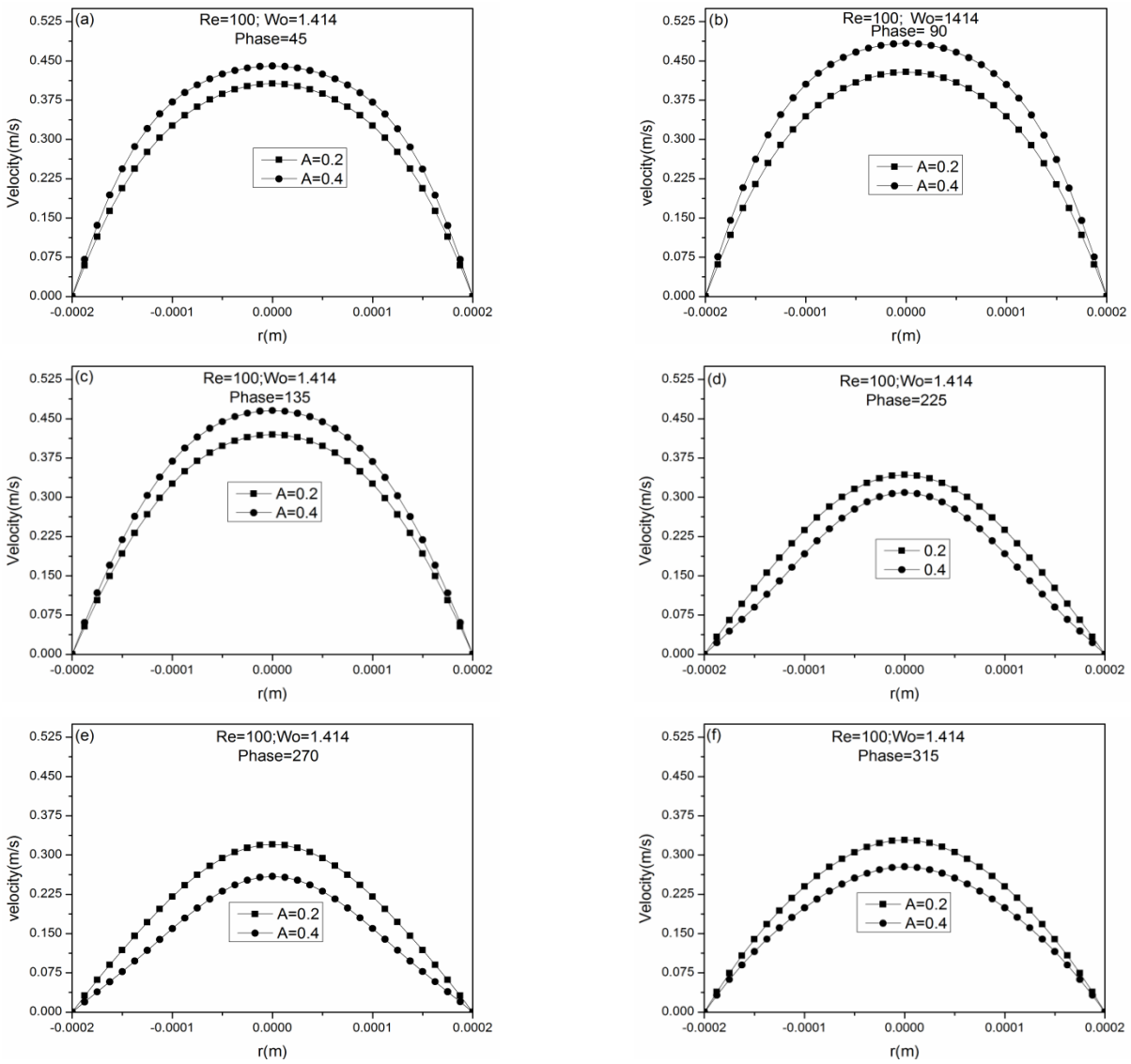

Fig. 4.1: Verification of velocity at two different amplitudes, for different phase angle.

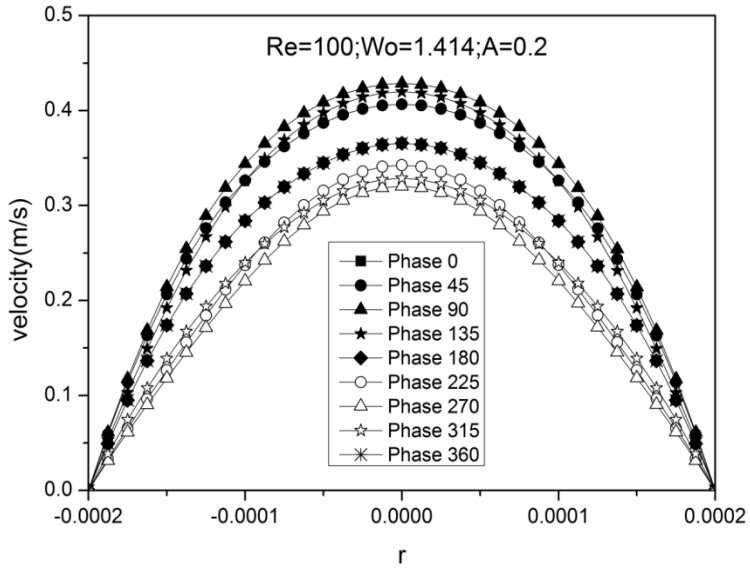

Fig. 4.2: Variation of velocity magnitude in radial direction for different phase angles (0-360)

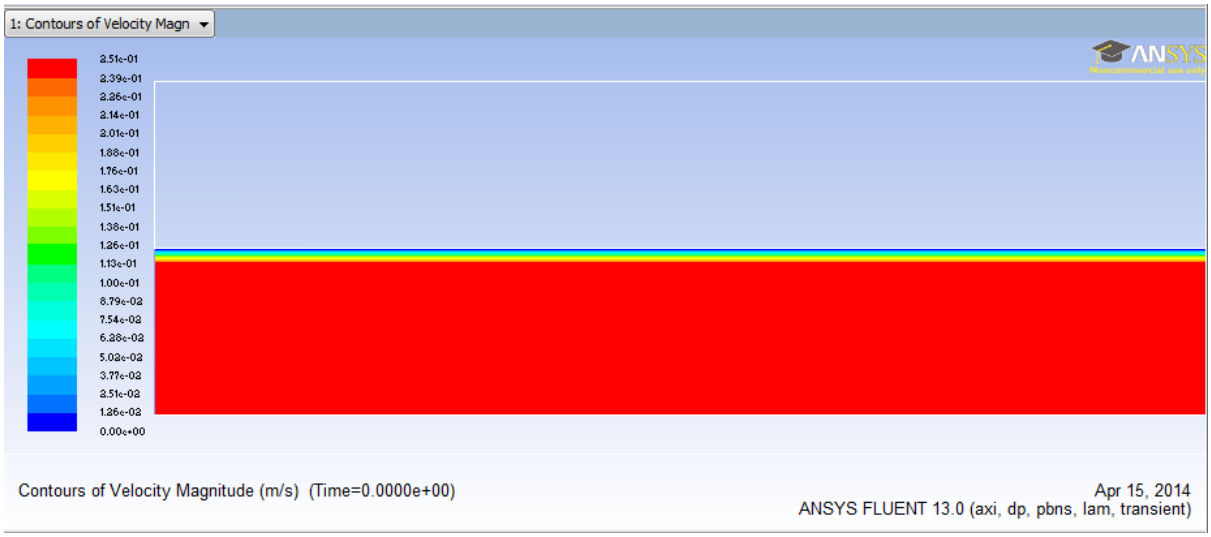

Figure 4.3(a): Contours of velocity magnitude before calculation in entrance region.

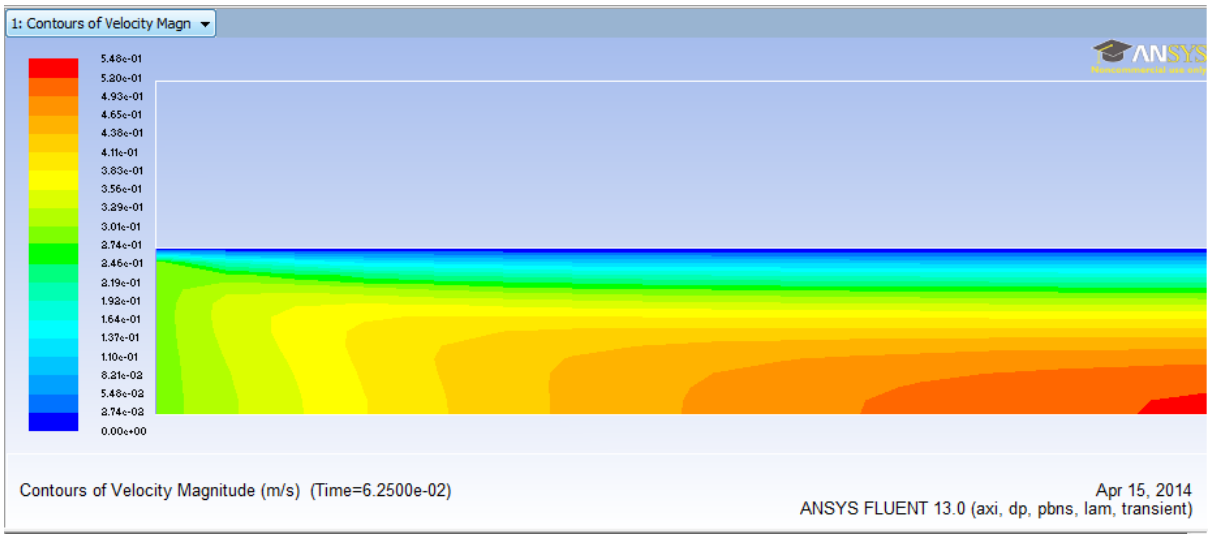

Figure 4.3(b): Contours of velocity magnitude at phase angle 45 in entrance region.

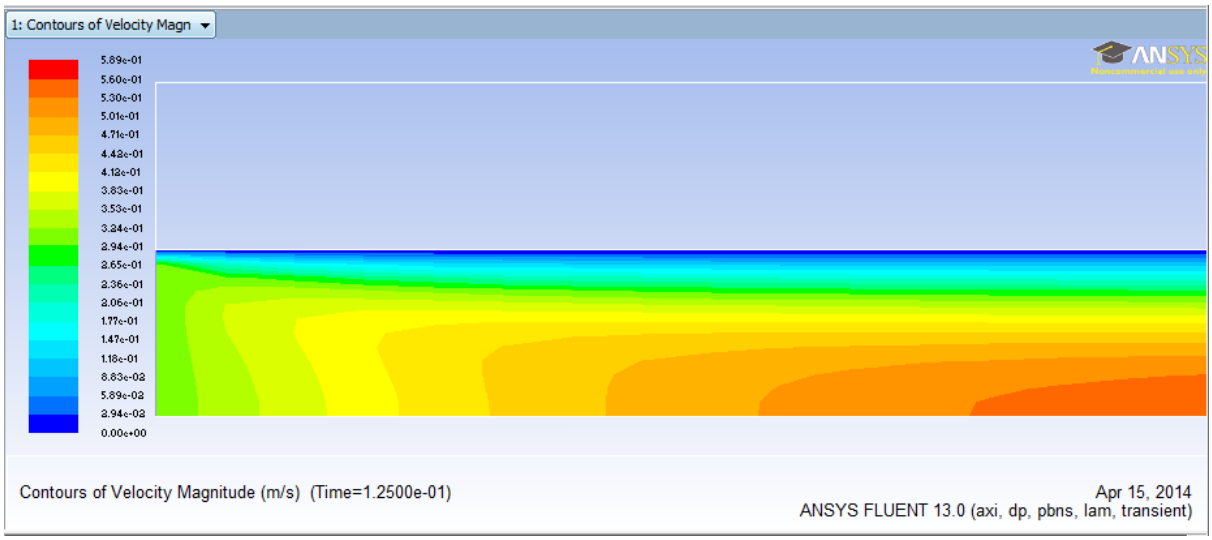

Figure 4.3(c): Contours of velocity magnitude at phase angle 90 in entrance region.

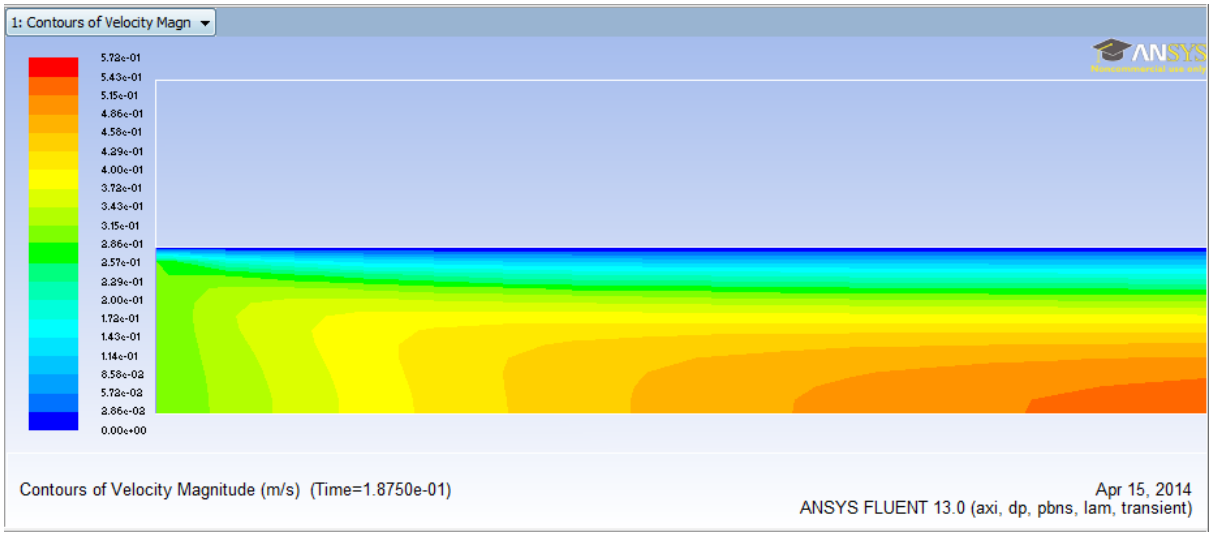

Figure 4.3(d): Contours of velocity magnitude at phase angle 135 in entrance region.

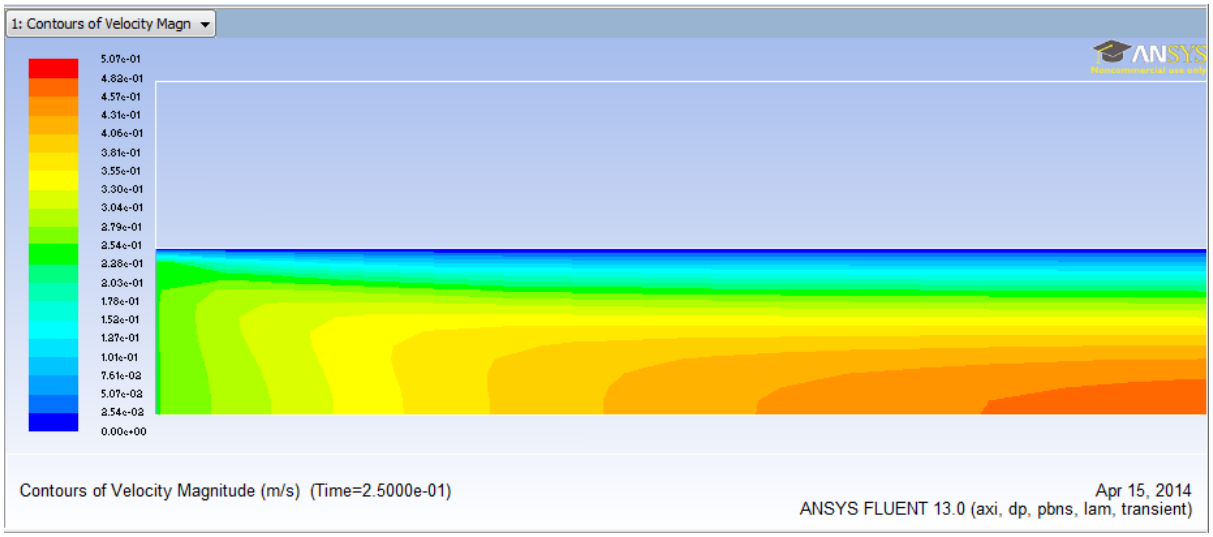

Figure 4.3(e): Contours of velocity magnitude at phase angle 180 in entrance region.

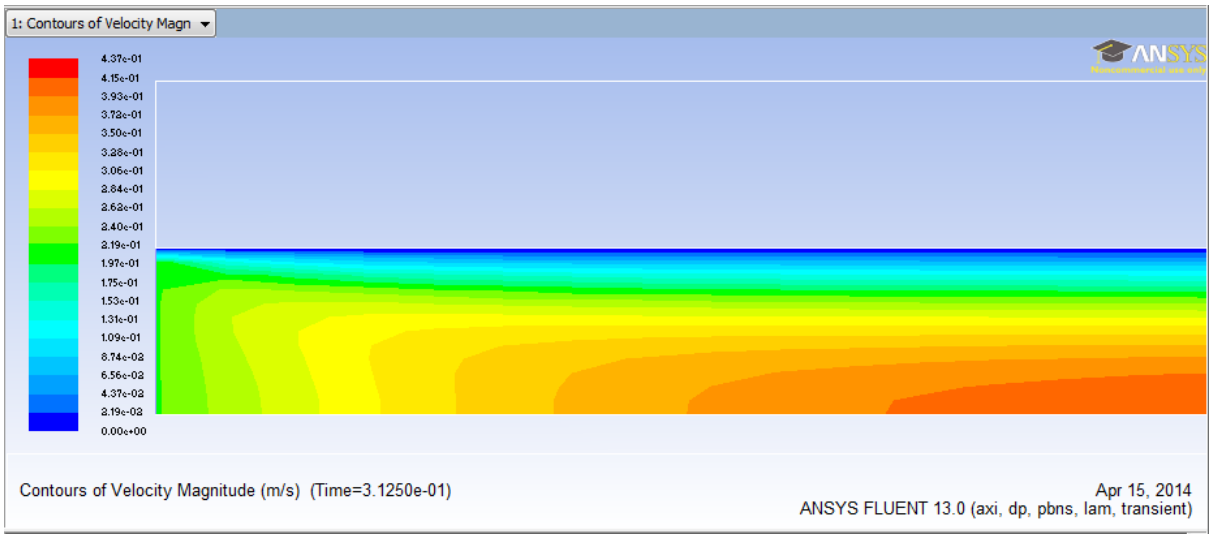

Figure 4.3(f): Contours of velocity magnitude at phase angle 225 in entrance region.

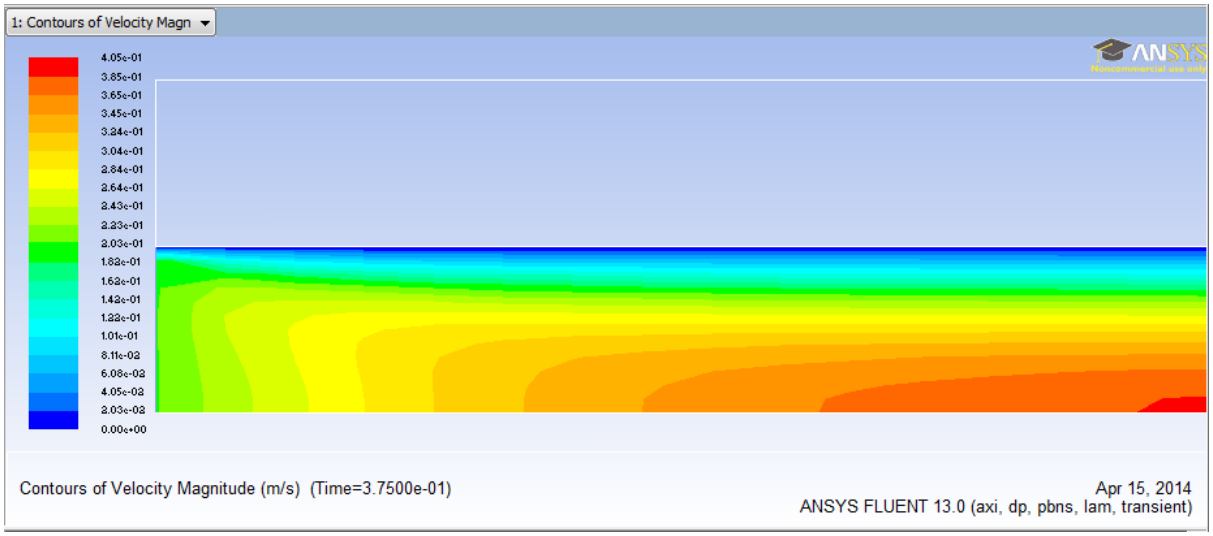

Figure 4.3(g): Contours of velocity magnitude at phase angle 270 in entrance region.

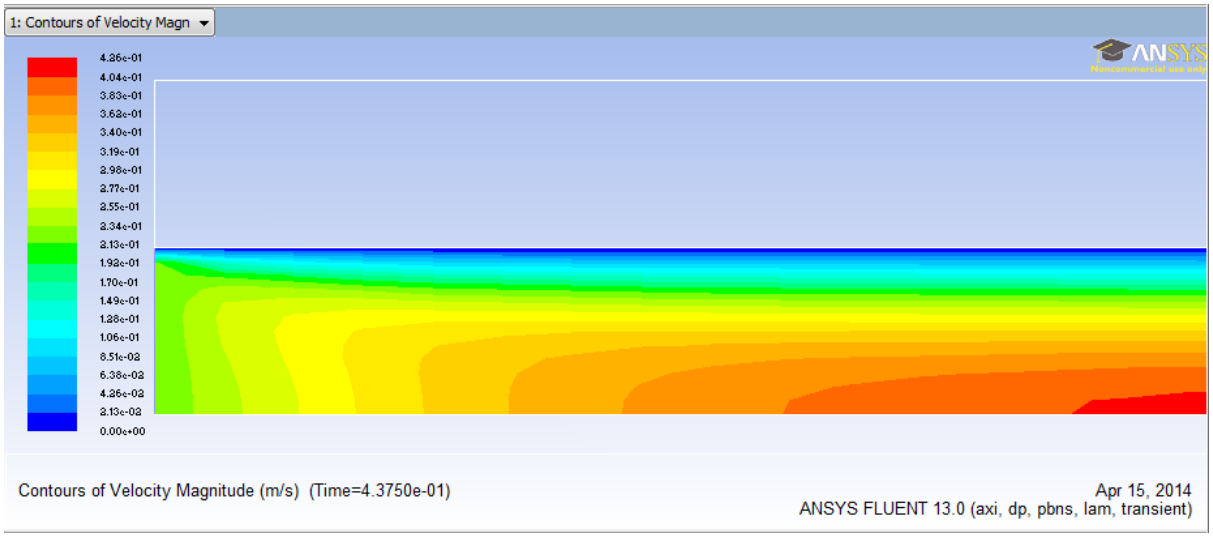

Figure 4.3(h): Contours of velocity magnitude at phase angle 315 in entrance region.

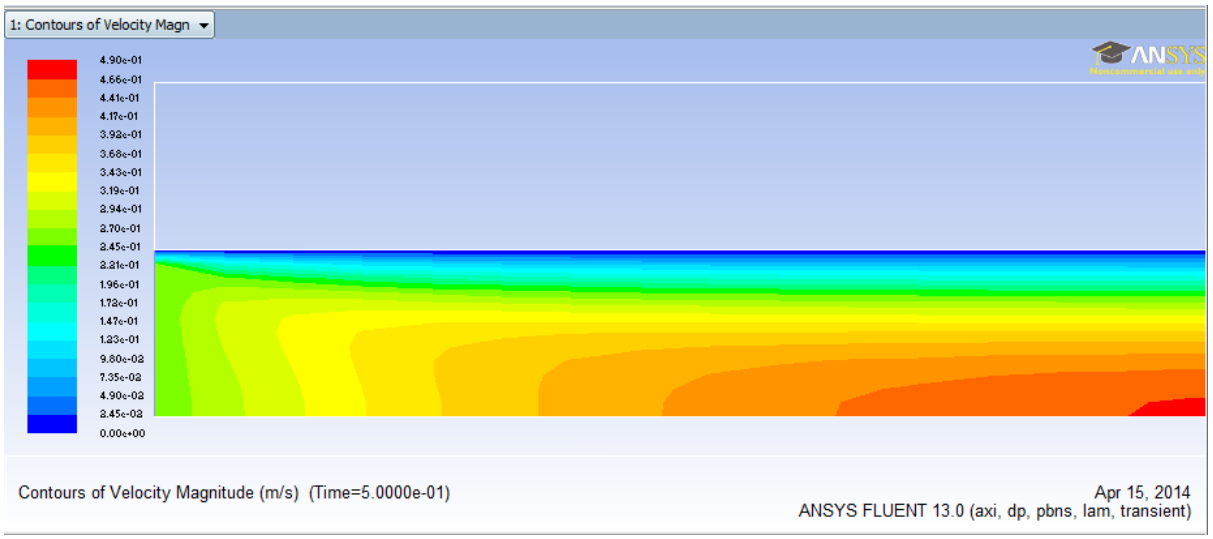

Figure 4.3(i): Contours of velocity magnitude at phase angle 360 in entrance region.

Contours of velocity magnitude in axial direction at the entrance region (developing zone) for different phase angles for a particular time period shown in Fig. 4.3 (a-i). From this it has been found that the hydrodynamic entrance length changes continuously over a cycle. Since the hydrodynamic boundary layer changes continuously over a cycle, thermal behavior may also affected by such pulsation.

By considering this, detail thermal analysis of simultaneously developing single phase laminar pulsating flow in a microtube is done. As the thermal conductivity ratio (k_{sf}) plays vital role in affecting axial wall conduction [31-38], simulations are carried out for different wall material such that k_{sf} varies in the range of 0.344 - 715.

The axial variation of dimensionless heat flux (ϕ) at the solid-fluid interface for different conductivity ratio represented as very lower (0.344, 2.3) lower (38.34), moderate (193.33) and higher (337.33, 715) k_{sf} values shown in Fig. 4.4. Since microtube wall having some finite thickness and because of conjugate heat transfer, it is not guaranteed that same heat flux which applied at the outer surface of the tube will experienced at the solid-fluid interface. The actual heat flux experienced at the solid-fluid interface control the heat transfer process. Three different phase angles (0, 90, and 270) at a frequency of f = 2 Hz (or Wo = 1.414) are considered in Fig. 4.4.

At very low k_{sf}, the actual heat flux experienced at the inner surface of the microtube is almost uniform in the axial direction as shown in Fig. 4.4(a) and Fig. 4.4(b). This is due to the fact that lower thermal conductivity ratio leads to higher thermal resistance in tube wall in the axial direction which qualitatively similar to zero thickness tube with constant heat flux applied. But with increasing the conductivity ratio, the actual heat flux experienced at the solid-fluid interface deviates from the ideal heat flux ($\overline{q}$) value supposed to experience at the interface. The effect is more pronounced at higher thermal conductivity ratio compared to moderate conductivity ratio (Fig. 4.4(c-f). This deviation is due to lower axial thermal resistance of the tube wall and at the inlet the effect of thermal boundary layer is dominated. By increasing the conductivity of tube wall material, dimensionless heat flux increases continuously in the entrance region leading to the accumulation of heat near the entrance of the microtube where more heat exchange will take place. It is due to the severe conjugate heat transfer and boundary layer effect.

With increasing phase angle from 0 to 90, the actual heat flux experienced at any location of the solid-fluid interface increases slightly. This is due to increase in instantaneous velocity (which is highest) when phase angle changes from 0 to 90. Again, by changing the

phase angle to 270, there is decrement of the flux (ϕ) compared to phase angle of 0. This is due to decrease in instantaneous velocity (which is lowest) when phase angle changes from 90 to 270. Thus, at higher pulsating velocity, the rate of heat transfer is higher and vice versa.

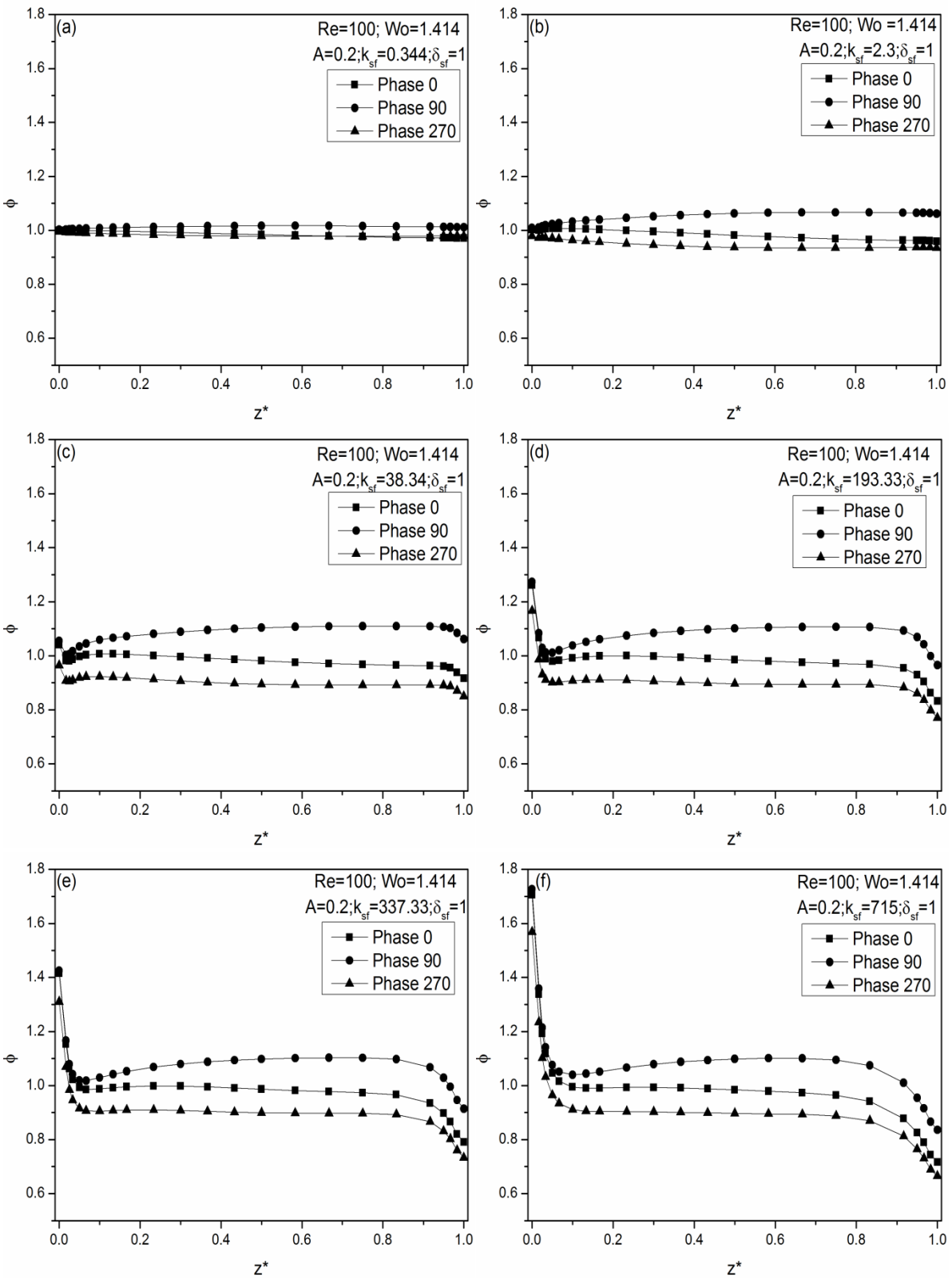

Fig. 4.4: Axial variation of dimensionless heat flux for different k_{sf} values.

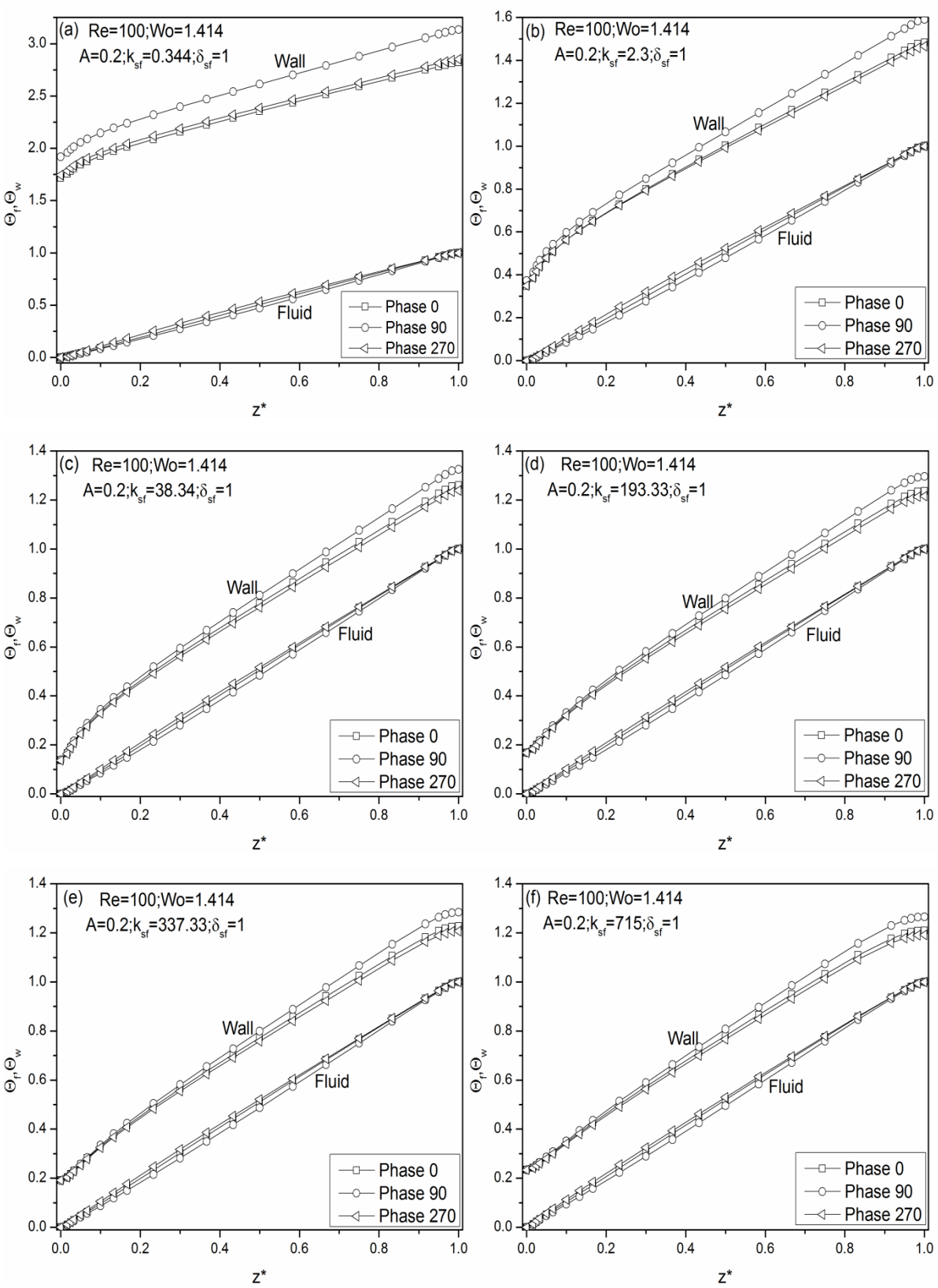

Fig. 4.5: Axial variation of dimensionless wall and bulk fluid temperature, for different k_{sf} values.

The axial variation of dimensionless wall temperature at the solid-fluid interface and the average bulk fluid temperature are shown in Fig. 4.5, which corresponds to Fig. 4.4. Generally bulk fluid temperature increases linearly from inlet to outlet in the case of constant heat flux boundary condition as the surface area exposed to heat transfer increases linearly in the flow direction. Again, wall temperature vary linearly in the flow direction in the fully developed region only and it is due to the fact that instantaneous local heat transfer coefficient remains constant in fully developed region.

For lower k_{sf} value, the average fluid temperature increases linearly in the flow direction from the inlet to the outlet, where as the wall temperature varies linearly in the fully developed region only, as per the conventional theory (see Fig. 4.5(a), 4.5(b) and 4.5(c)) described above. But at higher k_{sf} this conventional variation is not followed exactly (see Fig. 4.5(e) and Fig. 4.5(f)). This indicates that there is heat flow from downstream location to upstream location in the microtube solid wall by means of conduction (due to temperature difference) in a direction opposite to fluid flow. With the advancement of phase angle 0 to 90, the bulk fluid temperature decreases and wall temperature increases. Comparatively, the wall temperature increases at a higher rate than the bulk fluid temperature. Increase in wall temperature is more in case of very low thermal conductive material (Fig. 4.5(a) and 4.5(b)). Again by further increasing phase angle to 270, bulk fluid temperature increases from initial value where as wall temperature is decreased from the value correspond to temperature at zero phase angles.

The axial variation of instantaneous local Nusselt number is shown in Fig. 4.6, which corresponds to Fig. 4.4 and Fig. 4.5. From Fig. 4.6 (a-f) it can be observed that the instantaneous local Nusselt number Nu(z,t) in the fully developed region is lowest (at any phase angle) when k_{sf} is minimum i.e. 0.334 and 2.3 (see Fig. 4.6(a) and 4.6 (b)). Secondly, the effect of phase angle can be seen at very lower k_{sf} (see Fig. 4.6(a) and Fig.4.6 (b)) more clearly than at higher k_{sf} (see Fig. 4.6(c-f)) where it varies slightly in the developing region only. Again the fully developed Nu(z,t) at any location (irrespective of phase angle) first increases with increasing k_{sf} from 0.334 to 193.33, then decreases slightly when k_{sf} again increased to 337.33 to 715.

Axial variation of space average instantaneous Nusselt number [Nu(t)] at different phase angles for different k_{sf} values shown in Fig. 4.7 which correspond to Fig. 4.6. Fig. 4.7 (a) shows that with the increase in phase angle from 0-180 no appreciable change in space average instantaneous Nusselt number where as by further increase in phase angle 180-360 results in enhancement of Nu(t). With subsequent increase in k_{sf} values shows periodic

oscillation of Nu(t) over the cycle. By increasing phase angle from 0-180 (in positive half cycle), Nu(t) reduces while it increases by further increasing the phase angle from 180-360 (in negative half cycle). (See Fig. 4.7 (c-f)).

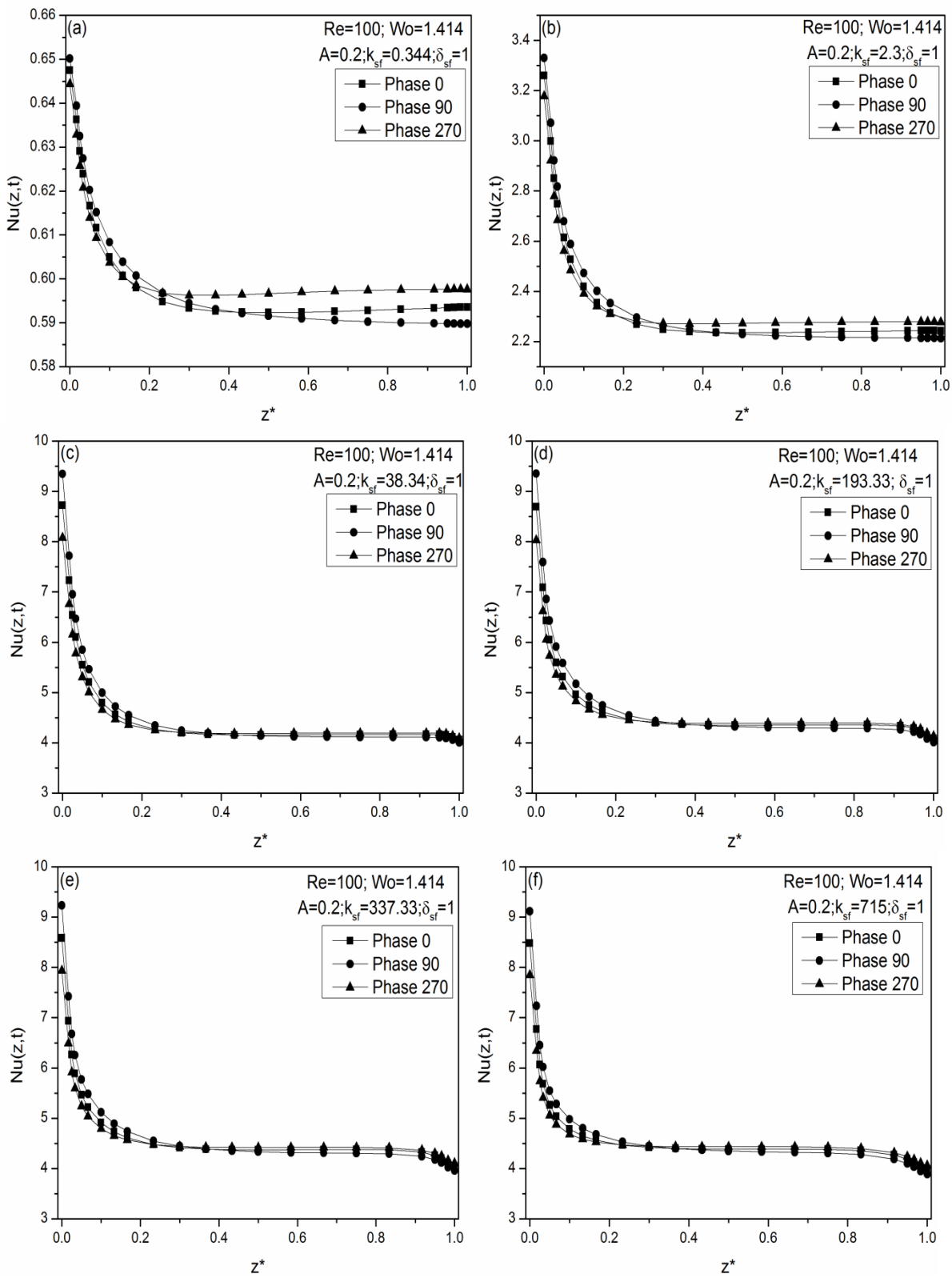

Fig. 4.6: Axial variation of instantaneous local Nusselt number for different k_{sf} values.

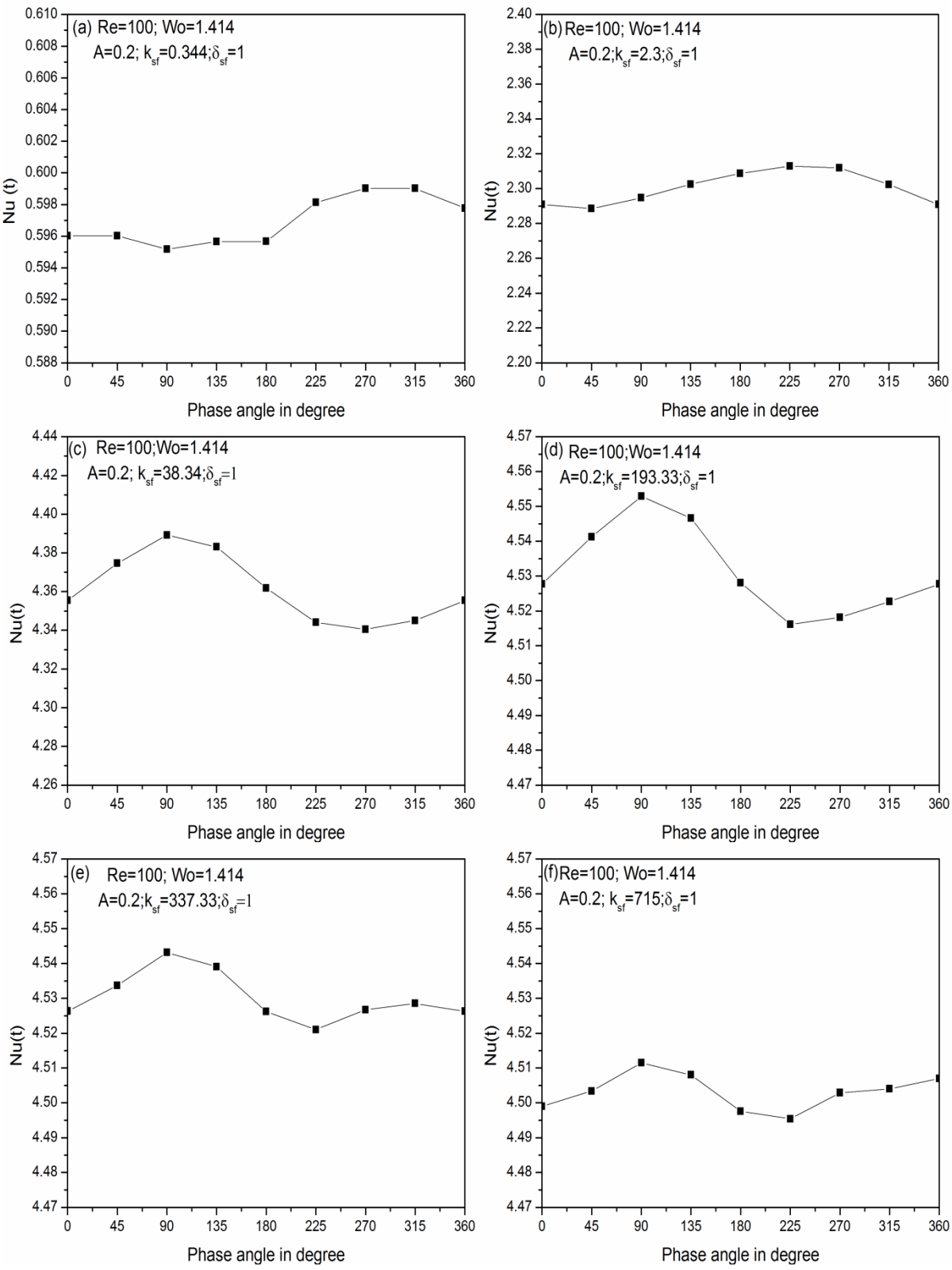

Fig. 4.7: Axial variation of space average instantaneous Nusselt number [Nu(t)] for different k_{sf} values.

Fig. 4.8 shows variation of time average relative Nusselt number over all the k_{sf} values ranging from 0.344-715. From this plot it is found that, for very lower k_{sf} values (0.344 and 2.3) time average relative Nusselt number [$Nu_r(z)$] remains almost constant along the entire length of microtube and its value is less than 1. It indicates that time average Nusselt number for unsteady case is less compared to its corresponding steady counterpart. By increasing k_{sf} values from 2.3 to 715, time average relative Nusselt number fluctuates over the entire length. In the entrance region it is less than one, increases gradually and fully devloped established region its value is more than one. It becomes almost uniform in the fully devloped region, except in the ending region.

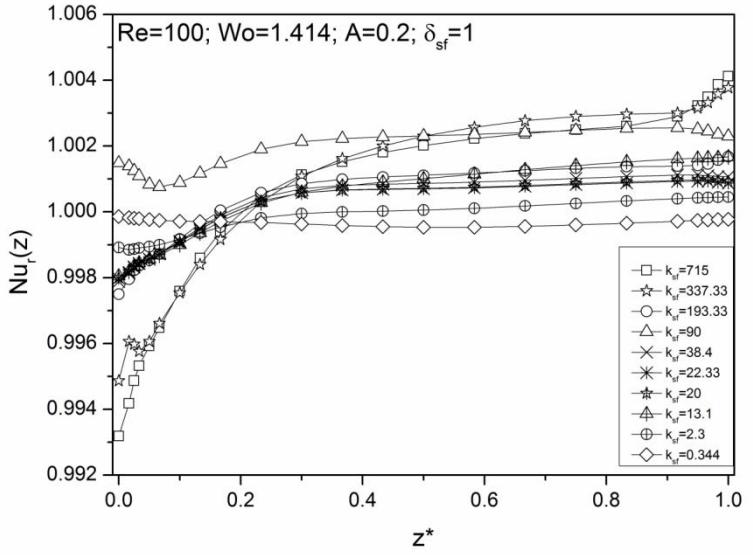

Fig.4.8: Variation of time average relative Nusselt number for all k_{sf} values

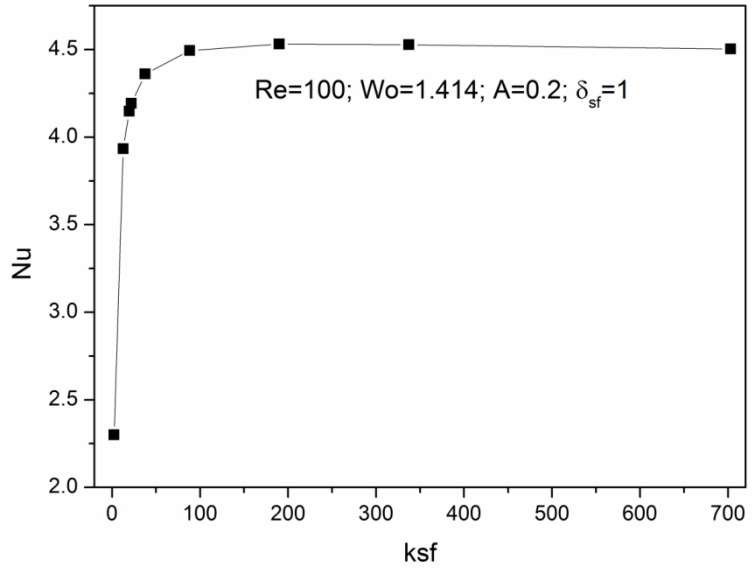

Fig 4.9: Variation of overall Nusselt number with k_{sf}

The discussion related to Fig. 4.6 indicates presence of an optimum value of k_{sf} at which the Nu(z) is maximum. This lead to Fig.4.9 where the k_{sf} values are varied in the range of 0.344 - 715, and the corresponding Nu are presented as a function of k_{sf} at a particular frequency (Wo = 1.414). With increasing k_{sf} values from a very small value of 0.344, the overall Nusselt number (Nu) increases at a very rapid rate up to a certain maximum value. After attaining maximum value, Nu decreases slightly with further increase in value of k_{sf}. But the downward slope of this decrease in Nu is comparatively very low. The decrease in overall Nusselt number at higher k_{sf} beyond a particular k_{sf} is primarily due to axial back conduction in the solid wall of the microtube. Thus, there exists an optimum value of solid to fluid conductivity ratio at which the overall Nusselt number is highest. This observation is in line with the previous study by Moharana et al. [33] and Tiwari et al. [36] where a steady flow was used.

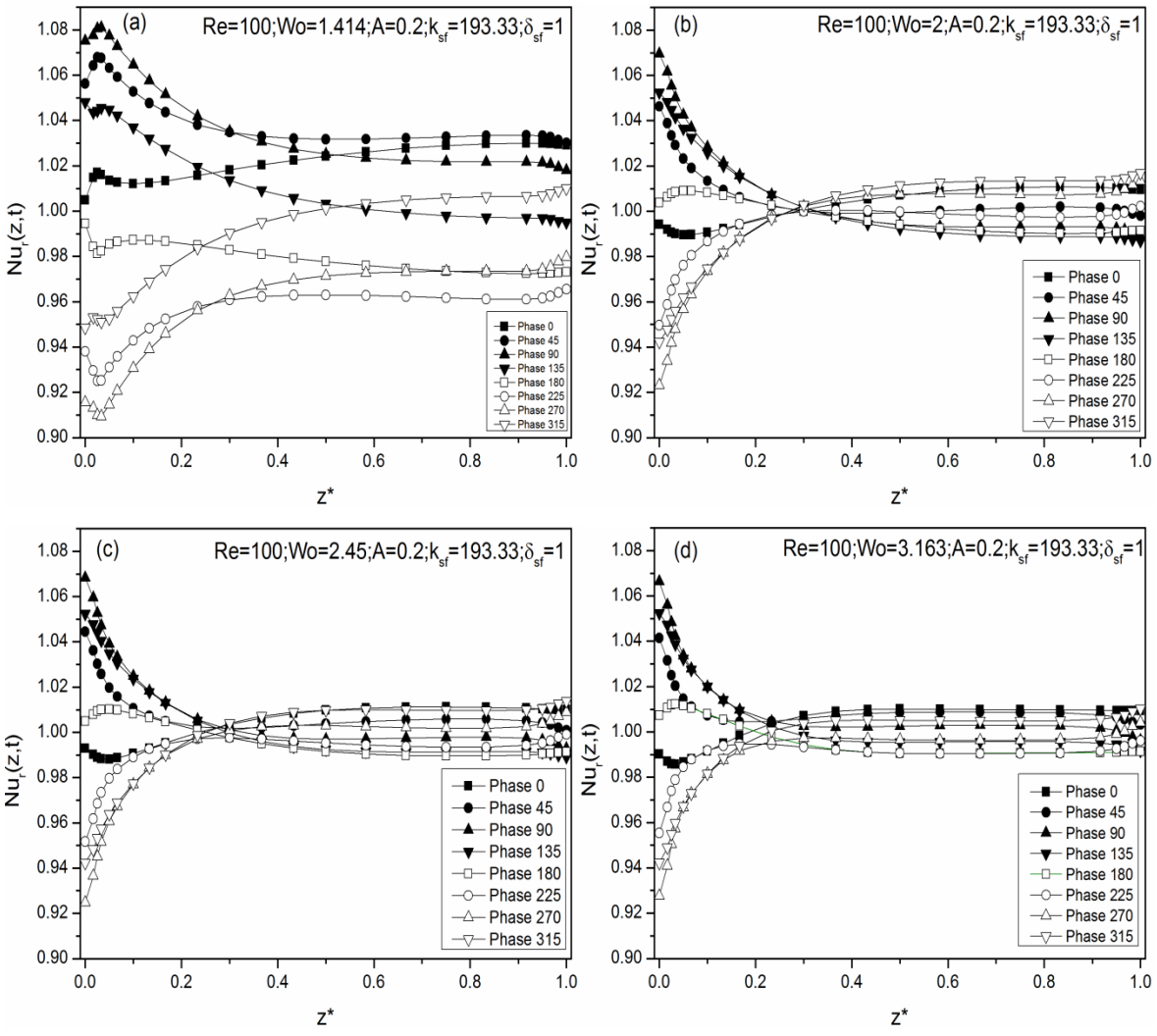

Fig. 4.10: Variation of relative instantaneous local Nusselt number at different frequency of pulsation for a particular k_{sf} = 193.33.

Variation of relative instantaneous local Nusselt number along the axial length at different frequency of pulsation for a particular k_{sf} = 193.33 is shown in Fig. 4.10. It has been found, relative instantaneous local Nusselt number oscillates over the axial length. (See Fig. 4.10(a-d)). Oscillations more pronounced at the entrance region where it decays in the developed region approaching towards the steady state Nusselt number. From Fig. 4.10, wider variation of relative Nusselt number is observed for lower pulsating frequency (Wo = 1.414) while at high pulsating frequency relative Nusselt number converge at some location and then diverged slightly in the fully developed region. (See Fig. 4.10 (b-d)).

The effect of pulsation frequency on time average relative Nusselt Number [$Nu_r(z)$] for very lower k_{sf} (0.344,2.3), lower k_{sf} (38.34), moderate k_{sf} (193.33) and at higher k_{sf} (337.33, 715) is represented in Fig. 4.11. To study such effect different pulsation frequencies are used, i.e. (f = 2, 4, 6 and 10 Hz). The corresponding Womersley numbers (Wo) are 1.414, 2, 2.45, and 3.163 respectively. Quantitatively, effect of pulsation frequency on heat transfer is very small. Therefore, to capture this small variation clearly, the term relative Nusselt number (Nu_r) is used.

It is found that the effect of pulsation frequency (Wo) is more pronounced in the entrance region, and by increasing pulsating frequency, the time average relative Nusselt number increases irrespective of k_{sf} values and its value is less than 1 indicating that heat transfer is less compared to its steady state. In the fully developed region effect is less and time average Nusselt number is slightly more than its corresponding steady state Nusselt number (for better clarification see Fig. 4.11(b) and 4.11 (e-f)).

At very low k_{sf}, there is increase in heat transfer by increasing pulsating frequency in the developed region (see Fig. 4.11 (a) and 4.11 (b)) compared to steady state, while at lower and moderate k_{sf} value (Fig. 4.11 (c) and 4.11(d)), no such effect is pronounced at pulsating frequency 2-6 Hz. At higher pulsating frequency (10 Hz) time average relative Nusselt number increases suddenly to a higher value in the fully developed region. But in case of moderate k_{sf} the time average relative Nusselt number goes to higher pick at 10 Hz frequency as compared to the lower k_{sf} values. At higher k_{sf}, value there is slight decrease in heat transfer compared to steady state by increasing pulsating frequency in the developed region (see Fig. 4. 11 (e) and 4.11 (f)).

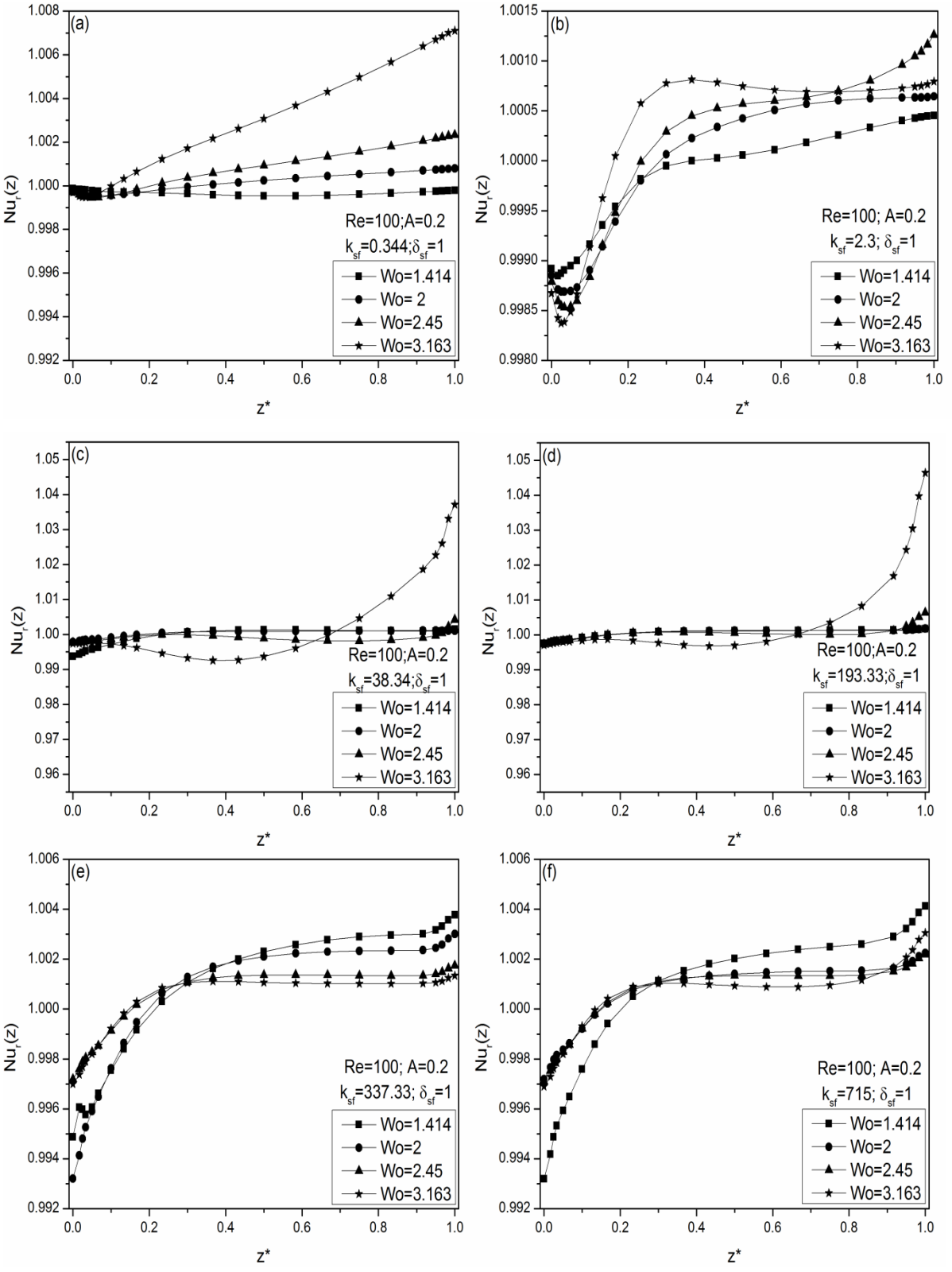

Fig. 4.11: Variation of time average relative Nusselt number at different pulsation frequency.

Chapter-5

Conclusion and future scope

A numerical analysis is carried out to highlight the effect of pulsation on axial wall conduction for the laminar flow in a microtube with constant heat flux boundary condition imposed on its outer surface. For this simulation, conductivity ratio is taken at a wide range (k_{sf} 0.344-715) while the thickness ratio (δ_{sf}), amplitude (A), and flow rate (Re) remain constant. To understand effect of pulsation, frequency of oscillation (f) is changed by taking four different Womersley numbers (1.414, 2, 2.45, and 3.163). Based on the numerical simulation, following conclusions are drawn:

- Due to the flow pulsation, highest velocity is observed for the phase angle 90 while lowest velocity is reported at 270 phase angle. Velocity profile overlaps for different phase angles (0, 180, and 360).
- For a particular pulsating frequency (Wo), with very low k_{sf} leads to lower the overall Nusselt number (Nu) while the time averaged relative Nusselt number remains [$Nu_r(z)$] almost constant through the entire length of microtube and it is less than the corresponding steady state Nusselt number.
- Moderate value of k_{sf} at a particular pulsation frequency (Wo) maximizes the overall Nusselt number.
- But at higher k_{sf}, with a particular frequency again lowers overall Nusselt number (Nu) slightly due to severe back conduction.
- For a particular pulsation frequency (Wo) there exists an optimum value of k_{sf} (moderate value of k_{sf}) at which overall Nusselt number (Nu) is maximum. Similar trend was observed by Moharana et al. [32] for a steady flow in square microchannel and circular microtube with constant heat flux as the boundary condition and Tiwari et al. [36] for steady flow in a microtube subjected to partial heating on its outer wall under constant heat flux as the boundary condition.

- ❖ Relative instantaneous local Nusselt number oscillates over the axial length for different phase angles. Oscillations more pronounced at the entrance region where it decays in the developed region approaching towards the steady state Nusselt number.
- ❖ Quantitatively, effect of pulsation frequency (Wo) on heat transfer is found to be very small.
- ❖ From the qualitative analysis, it is found that heat transfer increasing at lower thermal conductive microtube wall material (or k_{sf}) by increasing pulsating frequency.
- ❖ But with increasing pulsating frequency heat transfer rate reduces in case of higher thermal conductive material.

Review of literature indicates that pulsation (i) increases heat transfer (ii) decreases heat transfer, or (iii) no effect. The researchers actually failed to observe the present overall trend as none of the existing studies considered a widely varying thermal conductive wall material.

Since in most of the practical engineering applications, working fluid undergoes phase change, thermal analysis of pulsatile flow with multi-phase flow is one of the future scopes of this project. Apart from this, thermo-hydrodynamic analysis for a pulsatile flow can also be done for the turbulent flow having very high Reynolds number or low Reynolds number under the favorable conditions of turbulent flow. At some practical situations, tube wall may also subjected to constant wall temperature or partially heated instead of full heating. So, these requirements will initiates further work in the above project. It is expected that, this present work will give significant idea and create a path for new future work.

References:

1. Khandekar S. and Moharana M. K., Some Applications of Micromachining in Thermal-Fluid Engineering, Chapter in: Introduction to Micromachining, 2nd Edition, Editor: Dr. V. K. Jain, Narosa Publishing House, 2014.
2. Richardson E.G. and Tyler E., 1929, The transverse velocity gradient near the mouths of pipes in which an alternating or continuous flow of air is established, The Proceedings of the Physical Society, 42(1): pp. 1-15.
3. Uchida S., 1956, The pulsating viscous flow superposed on the steady laminar motion of incompressible fluid in a circular pipe, Zeitschrift für angewandte Mathematik und Physik ZAMP, 7(5): pp. 403-422.
4. Phillips E. M. and Chiang S.H., 1973, Pulsatile Newtonian frictional losses in a rigid tube, International Journal of Engineering Science, 11(6): pp. 579-589.
5. Muto T. and Nakane K., 1980, Unsteady flow in circular tube, Bulletin of JSME, 23 (186): pp. 1990-1996.
6. Kita Y., Hirose K. and Hayashi T., 1982, Heat transfer in pulsating laminar flow in a pipe, Bulletin of JSME, 25(200): pp. 217-224.
7. Creff R., Andre P. and Batina J., 1985, Dynamic and convective results for a developing laminar unsteady flow, International Journal for Numerical Methods in Fluids, 5(8): pp. 745-760.
8. Al-Haddad A. A. and Al-Binally N., 1989, Prediction of heat transfer coefficient in pulsating flow, International Journal of Heat and Fluid Flow, 10(2): pp. 131-133.
9. Havemann H. A. and Rao N. N. N., 1954, Heat transfer in pulsating flow, Nature, 174(4418): pp. 41.
10. Siegel R. and Perlmutter M., Heat transfer for pulsating laminar duct flow, 1962 Journal of Heat Transfer, 84(2): pp. 111-123.
11. Faghri M., Javdani K. and Faghri A., 1979, Heat transfer with laminar pulsating flow in a pipe, Letters in Heat and Mass Transfer, 6(4): pp. 259-270.
12. Karamercan O. E. and Gainer J. L., The effect of pulsations on heat transfer, 1979, Industrial and Engineering Chemistry Fundamentals, 18(1): pp. 11-15.
13. Mackley M. R., Tweddle G. M. and Wyatt I. D., 1990, Experimental heat transfer measurements for pulsatile flow in baffled tubes, Chemical Engineering Science, 45(5): pp. 1237–1242.

14. Cho H. W. and Hyun J. M., 1990, Numerical solutions of pulsating flow and heat transfer characteristics in a pipe, International Journal of Heat and Fluid Flow, 11(4): pp.321-330.
15. Kim S. Y., Kang B. H. and Hyun J. M., 1993, Heat transfer in the thermally developing region of a pulsating channel flow, International Journal of Heat and Mass Transfer, 36(17): pp. 4257-4266.
16. Guo Z. and Sung H. J., 1997, Analysis of the Nusselt number in pulsating pipe flow, International Journal of Heat and Mass Transfer, 40(10): pp. 2486-2489.
17. Moschandreou T. and Zamir M., 1997, Heat transfer in a tube with pulsating flow and constant heat flux, International Journal of Heat and Mass Transfer, 40(10): pp. 2461–2466.
18. Hemida H. N., Sabry M. N., Abdel-Rahim A. and Mansour H., 2002, Theoretical analysis of heat transfer in laminar pulsating Flow, International Journal of Heat and Mass Transfer, 45(8): pp. 1767-1780.
19. Habib M.A., Attya A.M., Eid A. I. and Aly A. Z., 2002, Convective heat transfer characteristics of laminar pulsating pipe air flow, Journal of Heat and Mass Transfer, 38 (3): pp. 221–232.
20. Zheng J., Zeng D., Wang P. and Gao H., 2004, An experimental study of heat transfer enhancement with a pulsating flow, Heat Transfer- Asian Research, 33(5): pp. 279–286
21. Yu J. C., Li Z. X. and Zhao T.S., 2004, An analytical study of pulsating laminar heat convection in a circular tube with constant heat flux, International Journal of Heat and Mass Transfer, 47(24): pp. 5297-5301.
22. Chattopadhyay H., Durst F. and Ray S., 2006, Analysis of heat transfer in simultaneously developing pulsating laminar flow in a pipe with constant wall temperature, International Communications in Heat and Mass Transfer, 33(4): pp. 475-481.
23. Elshafei E. A. M., Mohamed M. S., Mansour H. and Sakr M., 2007, Numerical study of heat transfer in pulsating turbulent air flow, Proceedings of Thermal Issues in Emerging Technologies, THETA 1, Cairo, Egypt, Jan 3-6th 2007: pp. 63-70.
24. Elshafei E. A. M., Mohamed M. S., Mansour H. and Sakr M., 2008, Experimental study of heat transfer in pulsating turbulent flow in a pipe, International Journal of Heat and Fluid Flow, 29(4): pp. 1029-1038.

25. Mehta B. and Khandekar S., 2010, Effect of periodic pulsations on heat transfer in simultaneously developing laminar flows: A numerical study, Proceedings of the International Heat Transfer Conference, IHTC14, August 08-13, 2010, Washington, DC, USA.
26. Jafari M., Farhadi M. and Sedighi K., 2013, Pulsating flow effects on convection heat transfer in a corrugated channel: A LBM approach, International Communications in Heat and Mass Transfer, 45: pp. 146-154.
27. Afrouzi H. H., Darzi A. A. R., Delavar M. A. and Mehrizi A. A., 2013, Pulsating flow and heat transfer in a helical tube with constant heat flux, International Journal of Advance Industrial Engineering, 1(2): pp. 36-39.
28. Maranzana G., Perry I. and Maillet D., 2004, Mini- and micro-channels: influence of axial conduction in the walls, International Journal of Heat and Mass Transfer, 47(17-18), pp. 3993–4004.
29. Zhang S. X., He Y. L., Lauriat G. and Tao W. Q., 2010, Numerical studies of simultaneously developing laminar flow and heat transfer in microtubes with thick wall and constant outside wall temperature, International Journal of Heat and Mass Transfer, 53(19–20): pp. 3977-3989.
30. Cole K. D. and Cetin B., 2011, The effect of axial conduction on heat transfer in a liquid microchannel flow, International Journal of Heat and Mass Transfer, 54, (11–12): pp. 2542–2549.
31. Moharana M. K., Agarwal G. and Khandekar S., 2011, Axial conduction in single-phase simultaneously developing flow in a rectangular mini-channel array, International Journal Thermal Sciences, 50(6): pp. 1001-1012.
32. Moharana M. K., Singh P. K. and Khandekar S., 2012, Optimum Nusselt number for simultaneously developing internal flow under conjugate conditions in a square microchannel, Journal of Heat Transfer, 134(7) 071703: pp. 01-10.
33. Moharana M. K. and Khandekar S., 2013, Numerical study of axial back conduction in microtubes, In Proceedings of the Thirty Ninth National Conference on Fluid Mechanics and Fluid Power, December 13-15, SVNIT Surat, Gujarat, India: Paper number FMFP2012 – 135.
34. Rahimi M. and Mehryar R., 2012, Numerical study of axial heat conduction effects on the local Nusselt number at the entrance and ending regions of a circular microchannel, International Journal Thermal Sciences, 59: pp. 87-94.

35. Moharana M. K. and Khandekar S., 2013, Effect of aspect ratio of rectangular microchannels on the axial back conduction in its solid substrate, International Journal of Microscale Nanoscale Thermal Fluid Transport Phenomena, 4(3-4): pp. 211-229.
36. Tiwari N., Moharana M.K., Sarangi S.K., 2013, Axial wall conduction in partially heated microtube, 40th National Conference on Fluid Mechanics and Fluid Power (FMFP2012), 12-14 December 2013, Hamirpur, India.
37. Kumar M. and Moharana M.K., 2013, Axial wall conduction in partially heated microtube, 22nd National and 11th International ISHMT-ASME Heat and Mass Transfer Conference, 28-31 December 2013, Kharagpur, India.
38. Hasan M. I., Hasan H. M. and Abid G. A., 2013, Study of the axial heat conduction in parallel flow microchannel heat exchanger, Journal of King Saud University-Engineering Sciences, 23: pp. 1-10.
39. Lin T. Y. and Kandlikar S. G., 2013, Heat transfer investigation of air flow in microtubes: Part II: Scale and axial conduction effects, Journal of Heat transfer, 135, (031704): pp. 1-6.
40. Persoons T., Saenen T., Donose R. and Baelmans M., 2009, Heat transfer enhancement due to pulsating flow in a microchannel heat sink, 15th International Workshop on Thermal Investigations of ICs and Systems (THERMINIC- 2009), 7-9 October, Leuven, Belgium.
41. Kumar N. and Agrawal A., 2009, Study of blood flow in microchannels, Proceedings ICCMS09, IIT Bombay, 1-5 December 2009: pp.1-2.
42. Tikekar M., Singh S. G. and Agrawal A., 2010, Measurement and modeling of pulsatile flow in microchannel," Microfluid Nanofluid, 9: pp. 1225-1240.
43. Persoons T., Saenen T., Oevelen T. V. and Baelmans M., 2012, Effect of flow pulsation on the heat transfer performance of a minichannel heat sink, Journal of Heat Transfer, 134(9) 091702: pp. 1-7
44. Nandi T. K. and Chattopadhyay H., 2013, Simultaneously developing flow in microchannels under pulsating inlet flow condition, International Journal of Transport Phenomena, 13(2): pp. 111-120.
45. Nandi T. K. and Chattopadhyay H., 2013, Numerical investigations of simultaneously developing flow in wavy microchannels under pulsating inlet flow condition, International Communications in Heat Mass Transfer, 47: pp. 27-31.

Publication out of this work

Mishra P. and Moharana M.K., Axial wall conduction in pulsating laminar flow in a microtube, 4th Joint US-European Fluids Engineering Division Summer Meeting and 12th International Conference on Nanochannels, Microchannels, and Minichannels, 3-7 August 2014, Chicago, USA. (Accepted for presentation).